

## 1           **Distinct explanations underlie gene-environment interactions in the UK Biobank**

2   Arun Durvasula<sup>1,2,3,4,5</sup> and Alkes L. Price<sup>4,5,6</sup>

- 3           1. Center for Genetic Epidemiology, Department of Population and Public Health Sciences,  
4           Keck School of Medicine, University of Southern California, Los Angeles, CA, USA  
5           2. Department of Genetics, Harvard Medical School, Cambridge, MA, USA  
6           3. Department of Human Evolutionary Biology, Harvard University, Cambridge, MA, USA  
7           4. Program in Medical and Population Genetics, Broad Institute of MIT and Harvard,  
8           Cambridge, MA, USA  
9           5. Department of Epidemiology, Harvard T.H. Chan School of Public Health, Boston, MA,  
10           USA  
11           6. Department of Biostatistics, Harvard T.H. Chan School of Public Health, Boston, MA,  
12           USA

13  
14   Correspondence: [arun.durvasula@med.usc.edu](mailto:arun.durvasula@med.usc.edu) or [aprice@hsph.harvard.edu](mailto:aprice@hsph.harvard.edu)

### 15           **Abstract**

16           The role of gene-environment (GxE) interaction in disease and complex trait architectures is  
17           widely hypothesized, but currently unknown. Here, we apply three statistical approaches to  
18           quantify and distinguish three different types of GxE interaction for a given trait and E variable.  
19           First, we detect locus-specific GxE interaction by testing for genetic correlation ( $r_g$ ) < 1 across E  
20           bins. Second, we detect genome-wide effects of the E variable on genetic variance by leveraging  
21           polygenic risk scores (PRS) to test for significant PRSxE in a regression of phenotypes on PRS,  
22           E, and PRSxE, together with differences in SNP-heritability across E bins. Third, we detect  
23           genome-wide proportional amplification of genetic and environmental effects as a function of the  
24           E variable by testing for significant PRSxE with no differences in SNP-heritability across E bins.  
25           Simulations show that these approaches achieve high sensitivity and specificity in distinguishing  
26           these three GxE scenarios. We applied our framework to 33 UK Biobank traits (25 quantitative  
27           traits and 8 diseases; average  $N=325K$ ) and 10 E variables spanning lifestyle, diet, and other  
28           environmental exposures. First, we identified 19 trait-E pairs with  $r_g$  significantly < 1 (FDR<5%)  
29           (average  $r_g=0.95$ ); for example, white blood cell count had  $r_g=0.95$  (s.e. 0.01) between smokers  
30           and non-smokers. Second, we identified 28 trait-E pairs with significant PRSxE and significant  
31           SNP-heritability differences across E bins; for example, BMI had a significant PRSxE for  
32           physical activity ( $P=4.6e-5$ ) with 5% larger SNP-heritability in the largest versus smallest  
33           quintiles of physical activity ( $P=7e-4$ ). Third, we identified 15 trait-E pairs with significant  
34           PRSxE with no SNP-heritability differences across E bins; for example, waist-hip ratio adjusted  
35           for BMI had a significant PRSxE effect for time spent watching television ( $P=5e-3$ ) with no  
36           SNP-heritability differences. Across the three scenarios, 8 of the trait-E pairs involved disease  
37           traits, whose interpretation is complicated by scale effects. Analyses using biological sex as the E  
38           variable produced additional significant findings in each of the three scenarios. Overall, we infer  
39           a significant contribution of GxE and GxSex effects to complex trait and disease variance.  
40             
41             
42             
43

## 44 Introduction

45

46 Although gene-environment (GxE) interactions have long been thought to impact the  
47 genetic architecture of diseases and complex traits<sup>1-4</sup>, the overall contribution of these effects  
48 remains unclear. Previous studies have detected GxE at a limited number of specific loci<sup>5-7</sup>  
49 (including studies that associated genotype to phenotypic variance without knowing the  
50 underlying E variable<sup>8-12</sup>). Previous studies have also proposed variance components methods  
51 for detecting genome-wide contributions of GxE to complex trait heritability<sup>13-18</sup>, but these  
52 methods have not been applied at biobank scale across a broad range of traits. Thus, the overall  
53 contribution of GxE to trait architectures is currently unknown. In addition, the relative  
54 importance of different types of GxE (e.g., locus-specific GxE, genome-wide effects of E on  
55 genetic variance, genome-wide effects of E on both genetic and environmental variance) is  
56 currently unclear. Studies of GxSex interaction face similar challenges<sup>19-24</sup>.

57

58 Here, we apply three statistical approaches to quantify and distinguish three different  
59 types of GxE interaction for a given trait and E variable. First, we detect locus-specific GxE  
60 interaction by testing for genetic correlation<sup>25</sup> ( $r_g$ ) < 1 across E bins. Second, we detect genome-  
61 wide effects of the E variable on genetic variance by leveraging polygenic risk scores<sup>26,27</sup> (PRS)  
62 to test for significant PRSxE<sup>28,29</sup> in a regression of phenotypes on PRS, E, and PRSxE, together  
63 with differences in SNP-heritability<sup>30-34</sup> across E bins. Third, we detect genome-wide  
64 proportional amplification of genetic and environmental effects as a function of the E variable by  
65 testing for significant PRSxE with no differences in SNP-heritability across E bins. We analyze  
66 33 traits from the UK Biobank<sup>35</sup> (25 quantitative traits and 8 diseases; average  $N=325K$ ),  
67 quantifying the contributions of each type of GxE effect across 10 E variables spanning lifestyle,  
68 diet, and other environmental exposures, as well as contributions of GxSex effects.

69

## 70 Results

71

### 72 *Overview of methods*

73

74 We aim to detect genome-wide GxE, i.e., GxE effects aggregated across the genome. We  
75 consider three potential scenarios that give rise to genome-wide GxE for a given trait and E  
76 variable (**Figure 1a**). In the first scenario (Imperfect genetic correlation), there is an imperfect  
77 genetic correlation across E bins due to different SNP effect sizes in different E bins. In the  
78 second scenario (Varying genetic variance), there are differences in SNP-heritability across E  
79 bins due to uniform amplification of SNP effect sizes across E bins; the environmental variance  
80 may either remain constant or vary across E bins. In the third scenario (proportional  
81 amplification), the genetic and environmental variance vary proportionately across E bins due to  
82 proportionate scaling of SNP effect sizes and environmental effect sizes across E bins, so that  
83 SNP-heritability remains the same across E bins. We conceptualize these three scenarios as  
84 acting at different levels in a hierarchy that leads from genetic variants to pathways to complex  
85 traits or disease (see **Discussion**).

86

87 The three scenarios can be formalized under the following model:

88

$$y_j = \sum_i x_{ij}\beta_i + \sum_i \gamma_i x_{ij}E_j + \sum_i \xi x_{ij}\beta_i E_j + \varepsilon_j + \eta \varepsilon_j E_j, \#(1)$$

89  
90 where  $y_j$  denotes the phenotype for individual  $j$ ,  $x_{ij}$  denotes the genotype of individual  $j$  at SNP  
91  $i$ ,  $\beta_i$  denotes the effect size of SNP  $i$ ,  $\gamma_i$  denotes SNP-specific GxE effects,  $E_j$  denotes the E  
92 variable value for individual  $j$ ,  $\xi$  quantifies the amplification of genetic effects across E values,  
93  $\varepsilon_j$  denotes environmental effects, and  $\eta$  quantifies the amplification of environmental effects  
94 across E values. In Scenario 1,  $\gamma_i$  will be nonzero. In Scenario 2,  $\xi$  will be nonzero. In Scenario  
95 3,  $\xi$  and  $\eta$  will be nonzero and equal.

96  
97 In this study, we apply three statistical approaches (**Figure 1b**) to UK Biobank data to  
98 detect genome-wide GxE, analyzing 33 traits (25 quantitative traits and 8 diseases; average  
99  $N=325K$ ) and 10 environmental variables as well as biological sex. First, we detect Imperfect  
100 genetic correlation (Scenario 1) by estimating the genetic correlation of effect sizes between sets  
101 of individuals binned on their E variables using cross-trait LD Score regression<sup>25</sup> (LDSC)  
102 (**Methods**). For non-binary E variables, we estimate the genetic correlation between the most  
103 extreme quintiles of the E variable; for binary E variables, we estimate the genetic correlation  
104 between individuals in each E bin. Second, we employ PRSxE regression<sup>28,29</sup>, defined as a  
105 regression of the phenotype on the PRS<sup>26,27</sup> multiplied by the E variable across individuals, to  
106 detect both Varying genetic variance (Scenario 2) and Proportional amplification (Scenario 3)  
107 (**Methods**); we note that PRSxE regression is not sensitive to changes in environmental variance  
108 only (**Methods**). We use PRS computed by PolyFun-pred<sup>27</sup> for all analyses involving PRS. We  
109 do not standardize the E variables, and we correct for main and interaction effects of several  
110 covariates (**Methods**). Finally, we distinguish between Scenario 2 and Scenario 3 by estimating  
111 the SNP-heritability within each E bin using BOLT-REML<sup>33</sup> and testing for significant  
112 differences between E bins (most extreme quintiles for non-binary E variables; each bin for  
113 binary E variables).

114  
115 We assign a trait-E pair to Scenario 1 if it has a genetic correlation across E bins  $< 1$   
116 (regardless of whether it differs in SNP-heritability or has a significant PRSxE regression term);  
117 we assign a trait-E pair to Scenario 2 if it has both a significant PRSxE regression term and a  
118 significant difference in SNP-heritability across E bins; finally, we assign a trait-E pair to  
119 Scenario 3 if it has a significant PRSxE regression term with no significant difference in SNP-  
120 heritability across E bins (**Figure 1c**). We note that for some trait-E pairs, we detected both  
121 locus-dependent GxE (Scenario 1) and non-locus-dependent GxE (Scenario 2 or Scenario 3). In  
122 the **Supplementary Note**, we provide interpretations of test outcomes that do not correspond to  
123 exactly one of the three scenarios. We estimate the excess trait variance explained by genome-  
124 wide GxE as follows. In Scenario 1, we transform the estimate of genetic correlation across E  
125 bins to the variance scale (**Methods; Supplementary Note**). In Scenario 2 and Scenario 3, we  
126 approximate the relative amount of trait variance explained by GxE effects (relative to the  
127 genetic variance) as the trait variance explained by PRSxE effects divided by the trait variance  
128 explained by the PRS; this approximation is valid under a model in which the PRSxE effects are  
129 proportional to the GxE effects (**Methods**). All reported variances are transformed to the liability  
130 scale for disease traits. We have released open-source software implementing the above  
131 approaches (see Code Availability), as well as their output from this study (see Data  
132 Availability).

133  
134  
135  
136  
137  
138  
139  
140  
141  
142  
143  
144  
145  
146  
147  
148  
149  
150  
151  
152  
153  
154  
155  
156  
157  
158  
159  
160  
161  
162  
163  
164  
165  
166  
167  
168  
169  
170  
171  
172  
173  
174  
175  
176  
177  
178

## Simulations

We performed simulations of the three Scenarios to evaluate the properties of the three statistical approaches. We assigned individuals to one of two E bins and simulated genetic effects at 10,000 causal SNPs based on the Scenario and E bin. We simulated sample sizes specific to each statistical approach to match our real data analyses (see below). In Scenario 1, we set the SNP-heritability to 25% and varied the genetic correlation from 99% to 94%. In Scenario 2, we set the genetic correlation to 100%, set the SNP-heritability to 25% in one E bin, and varied the SNP-heritability from 26% to 30% in the other E bin. In Scenario 3, we amplified the (genetic and environmental components of) phenotypes in one E bin by a range of values from 1.025 to 1.1. In each Scenario, we report the proportion of significant tests ( $P < 0.05$ , which is fairly similar to our significance threshold for real traits; see below) for each of our three approaches: Genetic correlation ( $N=67K$  individuals per E bin), PRSxE regression (training  $N=337K$ , testing  $N=49K$ ), and SNP-heritability by E ( $N=67K$  individuals per E bin). Because linkage disequilibrium (LD) does not impact GxE effects, we simulated genotypes without LD. We adjusted the methods used in our simulations accordingly. For Genetic correlation, we used cross-trait LD score regression in the special case of no LD<sup>25</sup>. For PRSxE regression, we used a simple shrinkage estimator in the special case of no LD to compute PRS. For SNP-heritability by E, we estimated SNP-heritability using LD score regression in the special case of no LD<sup>36</sup>. Further details of the simulation framework are provided in the **Methods** section.

In Scenario 1, the Genetic correlation approach reported a significant test in 93% of simulations when the true genetic correlation was 97% or smaller, whereas the PRSxE regression and SNP-heritability by E approaches were well-calibrated (**Figure 2a** and **Supplementary Table 1**). In Scenario 2, the PRSxE regression approach reported a significant test in 88% of simulations when the SNP-heritability difference was 4% or larger, and the SNP-heritability by E approach reported a significant test in more than 88% of simulations when the SNP-heritability difference was 2% or larger, whereas the Genetic correlation approach was well-calibrated (**Figure 2b** and **Supplementary Table 1**). In Scenario 3, the PRSxE regression approach reported a significant test in 88% of simulations when the proportional amplification was 1.075 or larger, whereas the Genetic correlation and SNP-heritability by E approaches were well-calibrated (**Figure 2c** and **Supplementary Table 1**). In null simulations (heritable trait with no GxE), all three statistical approaches were well-calibrated (**Supplementary Figure 1**).

We compared our framework with GxEMM<sup>16</sup>, a variance components-based framework that implements two GxE tests: 1) a test for polygenic GxE under homoskedasticity (GxEMM-Hom), and 2) a test for polygenic GxE under heteroskedasticity (GxEMM-Het). We note that GxEMM-Hom and GxEMM-Het do not precisely map to the 3 scenarios that we study here. In addition, because GxEMM is a variance components-based framework, it is currently unable to scale to biobank-sized datasets. We evaluated the performance of GxEMM on a sample size of 10,000 individuals, as in the simulations of ref. <sup>16</sup>. We evaluated our statistical approaches using matched sample sizes, with 5,000 individuals per binary E bin and 10,000 test individuals for PRSxE regression. We kept the training data set size the same as in our main simulations ( $N=337K$ ). In Scenario 1, the GxEMM-Hom test reported a similar proportion of significant tests as the Genetic correlation approach, whereas the GxEMM-Het test reported roughly half as many

179 significant tests (**Supplementary Figure 2**). In Scenario 2, the GxEMM-Het test was less  
180 powerful than the PRSxE regression and SNP-heritability by E approaches, whereas the  
181 GxEMM-Hom test was well-calibrated (**Supplementary Figure 2**). In Scenario 3, the GxEMM-  
182 Het test was less powerful than the PRSxE regression approach, whereas the GxEMM-Hom test  
183 was well-calibrated (**Supplementary Figure 2**). Thus, at sample sizes that permit computational  
184 tractability, GxEMM is generally less powerful than our framework (and cannot distinguish  
185 Scenario 2 and Scenario 3).

186  
187 Recognizing that “E variables” may be significantly heritable (see below), we tested  
188 whether E variables that are heritable and genetically correlated to the trait induce false positives  
189 in our PRSxE regression approach. We performed null simulations in which the E variable had  
190 SNP-heritability of 25% (matching the trait) and was 100% genetically correlated to the trait. We  
191 binned individuals based on the E variable and performed the PRSxE regression test. We  
192 determined that there was no inflation in test statistics (**Supplementary Figure 3**). Thus, the  
193 PRSxE regression is robust to E variables that are heritable and genetically correlated to the trait.

194  
195 Our framework also estimates the excess trait variance explained by GxE effects, beyond  
196 what is explained by additive effects (for brevity, we refer to this as variance explained). We  
197 determined that estimates of trait variance explained were accurate in each of Scenario 1  
198 (regression slope = 0.98; **Supplementary Figure 4a**), Scenario 2 (regression slope = 0.85;  
199 **Supplementary Figure 4b**), and Scenario 3 (regression slope = 1.05; **Supplementary Figure**  
200 **4c**). We note that in both Scenario 2 and Scenario 3, G effects are correlated with GxE effects, as  
201 a correlation between genetic variance ( $G^2$ ) and the E variable implies a correlation between G  
202 and GxE. Current variance components methods do not account for this correlation and may  
203 therefore produce biased estimates of variance explained by GxE; we have verified this in  
204 simulations (**Supplementary Table 2**). Here, we report the difference in variance explained by a  
205 model including an interaction term (PRS+PRSxE terms) over a base model (PRS only) that  
206 does not include an interaction term, which is robust to this correlation (**Methods** and  
207 **Supplementary Figure 4**).

208  
209 In summary, our simulations indicate that our statistical approaches attain high sensitivity  
210 and specificity in classifying trait-E pairs into the distinct scenarios of GxE considered here and  
211 produce accurate estimates of excess trait variance explained by GxE.

212  
213 *Identifying gene-environment interactions across 33 complex traits/diseases and 10 E variables*

214  
215 We analyzed individual-level data for  $N=384K$  unrelated European-ancestry individuals  
216 from the UK Biobank<sup>35</sup>. We selected 33 highly heritable (z-score for nonzero SNP-heritability<sup>36</sup>  
217  $> 6$ ) and relatively independent (squared genetic correlation<sup>25</sup>  $< 0.5$ ) traits and diseases  
218 (**Supplementary Table 3**). In addition, we selected 10 relatively independent E variables  
219 spanning lifestyle, diet, and other environmental exposures ( $r^2 < 0.1$ ; primarily from ref. <sup>14</sup>;  
220 **Supplementary Figure 5**; see **Methods**). We note that these E variables are all significantly  
221 heritable, although the heritability tends to be low (mean SNP-heritability = 6%, max SNP-  
222 heritability = 15%; **Supplementary Table 4**). We assessed statistical significance using a  
223 threshold of  $FDR < 5\%$  across traits and E variables for a given statistical test (see **Methods**); in

224 practice, this FDR threshold corresponded to a P-value threshold of  $\approx 0.01$ , which is fairly  
225 similar to our simulations.

226  
227 Trait-E pairs assigned to Scenario 1 (Imperfect genetic correlation) are reported in **Figure**  
228 **3a** and **Supplementary Table 5**. We identified 19 trait-E pairs with genetic correlation  
229 significantly less than 1 (FDR<5%; average genetic correlation: 0.95), implicating 12 of 33 traits  
230 (including 11 quantitative traits and 1 disease) and 9 of 10 E variables tested. The implicated  
231 traits included 9 blood cell and biochemistry traits, as well as height, BMI, and asthma. On  
232 average, these interactions explained 0.30% of trait variance across all quantitative traits and  
233 0.19% of observed-scale variance across all diseases analyzed. The lowest genetic correlation  
234 significantly less than 1 was 0.85 (se=0.06) for asthma x time spent watching television,  
235 explaining 1.5% of trait variance. The significant GxE interaction for BMI and smoking status  
236 (explaining 0.4% of trait variance) was consistent with results from ref. <sup>14</sup>. Trait-E pairs assigned  
237 to Scenario 2 (Varying genetic variance) are reported in **Figure 3b** and **Supplementary Table 5**.  
238 We identified 28 trait-E pairs with significant PRSxE interaction (FDR<5%) and a significant  
239 SNP-heritability by E test (FDR<5%), implicating 13 of 33 traits (including 6 quantitative traits  
240 and 7 diseases) and 9 of 10 E variables tested. On average, these interactions explained 0.13% of  
241 trait variance across all quantitative traits and 8.8% of observed-scale variance across all diseases  
242 analyzed; the latter value is highly relevant for prediction of disease risk on the observed scale  
243 but is unlikely to reflect liability-scale GxE variance (see below and **Discussion**). Because  
244 standard interaction tests can be anti-conservative due to unmodeled heteroskedasticity<sup>37</sup>, we  
245 repeated our PRSxE interaction analysis using Huber-White variance estimators<sup>38,39</sup> (**Methods**).  
246 We determined that results were highly concordant with our primary PRSxE interaction analysis  
247 (mean Pearson correlation in p-values for interaction across trait-E pairs: 97%; **Supplementary**  
248 **Table 6**), suggesting that our findings are not driven by unmodeled heteroskedasticity. Trait-E  
249 pairs assigned to Scenario 3 (Proportional amplification) are reported in **Figure 3c** and  
250 **Supplementary Table 5**. We identified 15 trait-E pairs with significant PRSxE interaction  
251 (FDR<5%) but a non-significant SNP-heritability by E test (FDR<5%), implicating 11 of 33  
252 traits (all quantitative traits) and 9 of 10 E variables tested. On average, these interactions  
253 explained 0.17% of trait variance across all quantitative traits and 0% of observed-scale variance  
254 across all diseases analyzed.

255  
256 We analyzed matched quantitative and disease traits in order to assess whether the large  
257 observed-scaled variances for diseases in Scenario 2 were recapitulated for the quantitative traits.  
258 We matched three diseases (type 2 diabetes, hypercholesterolemia, hypertension) to highly  
259 genetically correlated quantitative traits ( $r_g > 50\%$ ) (HbA1c, LDL, systolic blood pressure).  
260 First, for type 2 diabetes and HbA1c ( $r_g = 0.66$ ), of the 4 E variables assigned to Scenario 2 for  
261 type 2 diabetes (average observed-scale variance explained = 17% across 4 E variables;  
262 maximum of 18% for alcohol consumption), no E variable was assigned to Scenario 2 for HbA1c  
263 (**Supplementary Table 7**). Second, for hypercholesterolemia and LDL ( $r_g = 0.71$ ), of the 5 E  
264 variables assigned to Scenario 2 for hypercholesterolemia (average observed-scale variance  
265 explained = 6.2% across 5 E variables; maximum of 6.6% for physical activity), only 1 E  
266 variable was assigned to Scenario 2 for LDL (average variance explained = 0.01% across 5 E  
267 variables; non-significant for physical activity) (**Supplementary Table 7**). Third, for  
268 hypertension and systolic blood pressure ( $r_g = 0.80$ ), of the 2 E variables assigned to Scenario 2  
269 for hypertension (average observed-scale variance explained = 2.7% across 2 E variables;

270 maximum of 2.7% for time spent napping), no E variable was assigned to Scenario 2 for systolic  
271 blood pressure (**Supplementary Table 7**). Thus, the large observed-scaled variances for diseases  
272 in Scenario 2 were not recapitulated for the matched quantitative traits (see **Discussion**).

273

274 We checked whether any trait-E pairs were assigned to more than one Scenario. We  
275 determined that 2 trait-E pairs were assigned to both Scenario 1 and Scenario 2 (BMI x alcohol  
276 consumption and BMI x Townsend deprivation index); 0 trait-E pairs were assigned to both  
277 Scenario 1 and Scenario 3; and 0 trait-E pairs were assigned to both Scenario 2 and Scenario 3  
278 (which is not possible based on their definition). We also identified 108 trait-E pairs with a  
279 significant SNP-heritability by E test but non-significant PRSxE interaction (**Supplementary**  
280 **Table 8**); our primary interpretation is that this is due to changes in environmental variance  
281 rather than GxE interaction (**Methods**), but we cannot exclude the possibility that this is due to  
282 GxE interaction that we have incomplete power to detect.

283

284 Examples of quantitative trait-E pairs assigned to each scenario are reported in **Figure 4**  
285 and **Supplementary Table 9**. First, white blood cell count x smoking status was assigned to  
286 Scenario 1 (**Figure 4a**). The Genetic correlation approach estimated a genetic correlation  
287 between smokers and non-smokers of 0.95, which is significantly less than 1 ( $P=6.7e-7$ ;  $FDR <$   
288  $5\%$ ), explaining 0.5% of the variance of white blood cell count (vs. SNP-heritability of 30%). On  
289 the other hand, the PRSxE regression approach ( $P=0.46$ ) and SNP-heritability x E approach  
290 ( $P=0.39$ ) produced non-significant results. We note that smokers had 0.09 s.d. higher mean white  
291 blood cell count than non-smokers (T-test  $P<1e-16$ ), as previously reported<sup>40</sup>. Second, BMI x  
292 physical activity was assigned to Scenario 2 (**Figure 4b**). The PRSxE regression approach  
293 ( $P=4.6e-5$ ) and SNP-heritability x E approach (SNP-heritability of 0.38 for highest E quintile vs.  
294 0.33 for lowest E quintile;  $P<7e-4$ ) both produced significant results ( $FDR < 5\%$ ), explaining  
295 0.16% of the variance of BMI (vs. SNP-heritability of 33%). On the other hand, the genetic  
296 correlation approach produced a non-significant result ( $P=0.43$ ). We note that BMI and physical  
297 activity were correlated ( $r=-0.09$ ,  $P<1e-16$ ) as previously reported<sup>41</sup>. Third, WHRadjBMI x time  
298 spent watching television (TV time) was assigned to Scenario 3 (**Figure 4c**). The PRSxE  
299 regression approach produced a significant result ( $P=5e-3$ ;  $FDR < 5\%$ ), explaining 0.95% of the  
300 variance of WHRadjBMI. On the other hand, the genetic correlation approach ( $P=0.29$ ) and  
301 SNP-heritability x E approach ( $P=0.08$ ) produced non-significant results. We note that  
302 WHRadjBMI and TV time were correlated ( $r = 0.08$ ,  $P<1e-16$ ).

303

304 In summary, we detected GxE interaction in each of the three scenarios across the 33  
305 traits and 10 E variables analyzed. We estimate that these GxE effects explain 0.6% of trait  
306 variance across all quantitative traits and 9.0% of observed-scale variance across all diseases  
307 analyzed, compared to average SNP-heritability of 29% (s.e. 3% across traits).

308

### 309 *Identifying gene-sex interactions across 33 diseases/complex traits*

310

311 We analyzed the same 33 traits for GxSex interaction using the same 3 statistical  
312 approaches. Traits assigned to Scenario 1 (Imperfect genetic correlation) are reported in **Figure**  
313 **5a** and **Supplementary Table 10**. We identified 18 quantitative traits and 4 diseases with cross-  
314 sex genetic correlation significantly less than 1 ( $FDR<5\%$ ; average genetic correlation: 0.92),  
315 consistent with previous results<sup>22</sup>. On average, these interactions explained 2.6% of trait variance

316 across all quantitative traits and 2.4% of observed-scale variance across all diseases analyzed.  
317 The lowest significant genetic correlation was 0.66 for WHRadjBMI<sup>22</sup>, explaining 17% of trait  
318 variance. Traits assigned to Scenario 2 (Varying genetic variance) are reported in **Figure 5b** and  
319 **Supplementary Table 10**. We identified 6 quantitative traits and 6 diseases with significant  
320 PRSxSex interaction (FDR<5%) and a significant SNP-heritability by Sex test (FDR<5%). On  
321 average, these interactions explained 0.13% of trait variance across all quantitative traits and  
322 5.6% of observed-scale variance across all diseases analyzed; the latter value is highly relevant  
323 for prediction of disease risk on the observed scale but is unlikely to reflect liability-scale GxSex  
324 variance (see below and **Discussion**). Traits assigned to Scenario 3 (Proportional amplification)  
325 are reported in **Figure 5c** and **Supplementary Table 10**. We identified 8 quantitative traits and 0  
326 diseases with significant PRSxSex interaction (FDR<5%) but a non-significant SNP-heritability  
327 by Sex test (FDR<5%). On average, these interactions explained 0.06% of trait variance across  
328 all quantitative traits (a very small contribution) and 0% of observed-scale variance across  
329 diseases analyzed. Of the 30 traits implicated across three scenarios, we identified 7 traits  
330 assigned to both Scenario 1 and Scenario 2, and 5 traits assigned to both Scenario 1 and Scenario  
331 3 (**Supplementary Table 10**). We also identified 2 traits with a significant SNP-heritability x  
332 Sex test but non-significant PRSxSex interaction (**Supplementary Table 11**); our primary  
333 interpretation is that this is due to changes in environmental variance rather than GxSex  
334 interaction (**Methods**).

335  
336 We again analyzed matched quantitative and disease traits to assess whether the large  
337 observed-scaled variances for diseases in Scenario 2 were recapitulated for the quantitative traits.  
338 First, for type 2 diabetes and HbA1c ( $r_g = 0.66$ ), type 2 diabetes was assigned to Scenario 2  
339 (observed-scale variance explained = 15%), but HbA1c was not assigned to Scenario 2  
340 (**Supplementary Table 12**). Second, for hypercholesterolemia and LDL ( $r_g = 0.71$ ),  
341 hypercholesterolemia was assigned to Scenario 2 (observed-scale variance explained = 5.9%),  
342 and LDL was also assigned to Scenario 2 but with much lower variance explained (0.56%)  
343 (**Supplementary Table 12**). Third, for hypertension and systolic blood pressure ( $r_g = 0.80$ ),  
344 hypertension was assigned to Scenario 2 (observed-scale variance explained = 2.5%), and  
345 systolic blood pressure was also assigned to Scenario 2 but with much lower variance explained  
346 (0.50%) (**Supplementary Table 12**). Thus, the large observed-scaled variances for diseases in  
347 Scenario 2 were not recapitulated for the matched quantitative traits (see **Discussion**).

348  
349 Examples of quantitative traits with significant GxSex assigned to each Scenario are  
350 reported in **Figure 6** and **Supplementary Table 13**. First, neuroticism score was assigned to  
351 Scenario 1 (**Figure 6a**). The Genetic correlation approach estimated a cross-sex genetic  
352 correlation of 0.90, which is significantly less than 1 ( $P=3.5e-9$ ;  $FDR < 5\%$ ), explaining 5.0% of  
353 the variance of neuroticism score. On the other hand, the PRSxSex regression approach ( $P=0.58$ )  
354 and SNP-heritability by Sex approach ( $P=0.45$ ) produced non-significant results. We note that  
355 males had lower prevalence of neuroticism than females (1.6% vs. 2.3% in top score for  
356 neuroticism,  $P<1e-16$ ), as previously reported<sup>42</sup>. Second, systolic blood pressure was assigned to  
357 Scenario 2 (**Figure 6b**). The PRSxSex regression approach ( $P=3.8e-5$ ) and SNP-heritability by  
358 Sex approach (SNP-heritability of 32% for males and 27% for females;  $P=2e-15$ ) both produced  
359 significant results ( $FDR < 5\%$ ), explaining 0.14% of the variance of systolic blood pressure (vs.  
360 SNP-heritability of 28%). In addition, the genetic correlation approach produced a significant  
361 result ( $P=7e-5$ ), explaining 2.5% of the variance of systolic blood pressure (Scenario 1); this



362 implies that multiple types of GxSex interaction impact systolic blood pressure. We note that  
363 males had higher systolic blood pressure than females ( $P < 2e-16$ ), as previously reported<sup>43</sup>. Third,  
364 HDL cholesterol was assigned to Scenario 3 (**Figure 6c**). The PRSxSex regression approach  
365 produced a significant result ( $P < 2e-16$ ;  $FDR < 5\%$ ), explaining 0.4% of the variance of HDL  
366 cholesterol. On the other hand, the SNP-heritability by Sex approach ( $P = 0.09$ ) was not  
367 significant. However, the genetic correlation approach estimated a cross-sex genetic correlation  
368 of 0.93, which is significantly less than 1 ( $P = 5e-6$ ;  $FDR < 5\%$ ), explaining 3.5% of the variance  
369 of HDL cholesterol (Scenario 1); this implies that multiple types of GxSex interaction impact  
370 HDL cholesterol. We note that males had 0.83 s.d. lower HDL cholesterol than females ( $P < 1e-$   
371  $16$ ).

372  
373 In summary, we detected GxSex interaction in each of the three scenarios across the 33  
374 traits analyzed. We estimate that these GxSex effects explain 2.8% of trait variance across all  
375 quantitative traits and 8.0% of observed-scale variance across all diseases analyzed, compared to  
376 average SNP-heritability of 29% (s.e. 3%).

## 377 378 **Discussion**

379  
380 We have applied three statistical approaches to detect, quantify, and distinguish the genome-  
381 wide contributions of three different types of GxE interaction (**Figure 1a**) across 33 UK Biobank  
382 traits, analyzing 10 E variables spanning lifestyle, diet, and other environmental exposures as  
383 well as biological sex. We determined that GxE interactions (involving these E variables) and  
384 GxSex interactions each explained a significant fraction of phenotypic variance, representing an  
385 appreciable contribution to trait architectures. It is possible that GxE interactions involving E  
386 variables not studied here could explain even more phenotypic variance. However, the much  
387 higher (observed-scale) variance explained by GxE and GxSex effects (in Scenario 2) for disease  
388 traits than for quantitative traits is complicated by scale effects (see below).

389  
390 Our finding of distinct explanations underlying GxE interactions (**Figure 1a**) motivates a  
391 unified model consistent with this finding. We propose a model in which GxE occurs at different  
392 levels of a hierarchy that leads from genetic variants to pathways to complex traits or disease  
393 (**Supplementary Figure 6**). In this model, Scenario 1 (Imperfect genetic correlation) occurs  
394 when an E variable modifies the effects of individual variants (or sets of variants), differentially  
395 impacting different parts of the genome; Scenario 2 (Varying genetic variance) occurs when an E  
396 variable modifies all of the pathways underlying genetic risk, uniformly impacting genetic  
397 variance; and Scenario 3 (Proportional amplification) occurs when an E variable modifies all  
398 aspects of trait biology, proportionately impacting both genetic and environmental variance.  
399 Under this model, an E variable can modify any point along the hierarchy from genetic variants  
400 to pathways to complex traits or disease. Further investigation and validation of this model is a  
401 direction for future research.

402  
403 Our study represents an advance over previous studies investigating genome-wide GxE.  
404 First, we distinguish three different types of GxE interaction: Imperfect genetic correlation,  
405 Varying genetic variance, and Proportional amplification (**Figure 1a**; also see **Supplementary**  
406 **Figure 6**). Second, most variance components methods for detecting genome-wide GxE<sup>13–15,17,18</sup>  
407 cannot detect genome-wide GxE unless SNP-heritability varies across E bins (Scenario 2). An

408 exception is GxEMM<sup>16</sup>, which detects other types of GxE by explicitly modeling genetic and  
409 environmental variance that varies with the E variable; however, GxEMM is less  
410 computationally tractable and generally less powerful than our framework (**Supplementary**  
411 **Figure 2**). Third, variance components methods that assume independence between G and GxE  
412 effects are susceptible to bias if G and GxE effects are correlated, but our statistical approaches  
413 are robust to this possibility (**Supplementary Figure 4**). Fourth, previous methods have not been  
414 applied at biobank scale across a broad range of traits; the statistical approaches that we propose  
415 are computationally scalable to very large data sets (see **Methods**), enabling our biobank-scale  
416 analyses implicating 60 trait-E pairs with significant GxE and 30 traits with significant GxSex.  
417 Fifth, a recent study reported that GxSex acts primarily through amplification<sup>24</sup> (Scenario 2 and  
418 Scenario 3), but our analyses of GxSex determined that Imperfect genetic correlation (Scenario  
419 1) explained a larger proportion of trait variance than amplification; in addition, ref.<sup>24</sup> did not  
420 estimate contributions to trait variance and did not distinguish between Scenario 2 and Scenario  
421 3, as we do here.

422  
423 Our study has several implications. First, our results narrow the search space of traits and E  
424 variables for which genome-wide association studies of GxE interactions are most likely to be  
425 fruitful; in particular, trait-E pairs with substantial trait variance explained by Scenario 1  
426 (Imperfect genetic correlation) (**Supplementary Table 5**) should be prioritized for locus-specific  
427 analyses, in preference to trait-E pairs with trait variance explained by Scenario 2 or Scenario 3.  
428 Second, our results imply that there is broad potential to improve polygenic risk scores (PRS) by  
429 leveraging information on E variables in training and/or test samples<sup>44</sup>. Third, there is broad  
430 potential to prioritize individuals for which a lifestyle intervention to modify an E variable would  
431 be most effective based on their genetic profile. Fourth, previous work has suggested that  
432 population-specific causal effect sizes in functionally important regions may be caused by  
433 GxE<sup>45</sup>, motivating efforts to partition the imperfect genetic correlations across E bins that we  
434 have identified across functionally important regions. Fifth, the significant contribution of GxE  
435 to trait architectures—even when restricting to the limited set of E variables that we analyzed  
436 here—implicates GxE effects as a factor in “missing heritability”, defined as the gap between  
437 estimates of SNP-heritability<sup>30</sup> and estimates of narrow-sense heritability<sup>46</sup> (e.g. from twin  
438 studies<sup>47</sup>); although GxE effects are not included in the *definition* of narrow-sense heritability,  
439 they can inflate twin-based *estimates* of narrow-sense heritability, analogous to GxG effects<sup>48</sup>.  
440 All of these implications motivate directions for future research.

441  
442 Our study has several limitations. First, our analyses assess GxE and GxSex interaction for  
443 disease traits on the observed scale (and then transform estimates to the liability scale),  
444 consistent with prevailing approaches for variance component analysis of disease traits<sup>31–34</sup>. Our  
445 analyses of matched quantitative and disease traits (**Supplementary Table 7**, **Supplementary**  
446 **Table 12**) strongly suggest that the much higher (observed-scale) variance explained by GxE and  
447 GxSex effects (in Scenario 2) for disease traits than for quantitative traits (**Supplementary**  
448 **Table 14**; also see **Figure 3b** and **Figure 5b**) is a consequence of analyzing disease traits on the  
449 observed scale, and unlikely to reflect liability-scale GxE or GxSex variance; directly modeling  
450 GxE or GxSex interaction on the liability scale<sup>50,51</sup> is an important direction for future research.  
451 Nonetheless, these observed-scale interactions are likely to be highly relevant for prediction of  
452 disease risk on the observed scale. Second, the E variables that we analyzed comprise an  
453 extremely limited subset of the set of E variables that may contribute to GxE effects (and their

454 values may be subject to measurement error); even when GxE effects are detected, the  
455 implicated E variable may be tagging an unmeasured causal E variable with larger GxE effects.  
456 Third, our use of PRSxE regression to detect GxE is limited by the accuracy of PRS and may  
457 require larger training sample sizes (enabling more accurate PRS) to be well-powered,  
458 particularly for less heritable traits. The average accuracy of the PRS across traits in the held-out  
459 set of 49K individuals was 9.2%, as measured by  $r^2$  between predicted and true phenotypes  
460 (**Supplementary Table 3**). Fourth, our estimates of the trait variance explained by GxE effects  
461 detected via PRSxE analyses assume that PRSxE effects extrapolate linearly to GxE effects  
462 (**Methods**); we believe that this is a reasonable assumption, but we cannot formally exclude the  
463 possibility that genetic effects captured by PRS interact differently with an E variable than  
464 genetic effects not captured by PRS. Fifth, most of the E variables that we study are weakly  
465 heritable (**Supplementary Table 4**), raising the possibility of GxG (rather than GxE) effects; we  
466 consider GxG to be an unlikely explanation given the E variables' low SNP-heritabilities, but we  
467 cannot formally exclude this possibility. Sixth, our use of PRSxE regression to detect GxE may  
468 be anti-conservative due to unmodeled heteroskedasticity<sup>37</sup>; however, we obtained nearly  
469 identical results using Huber-White variance estimators (also known as robust regression<sup>38,39</sup>)  
470 (**Supplementary Table 6**), suggesting that this does not impact our findings. We note that we  
471 observe many instances of differences in trait variance across E variables (**Supplementary**  
472 **Table 8**), but these alone are not indicative of GxE interactions. Seventh, our use of PRSxE  
473 regression to detect GxE may produce false positives if there is a nonlinear relationship between  
474 E and trait value; we included an  $E^2$  term in PRSxE regressions to ameliorate this possibility but  
475 determined that inclusion or exclusion of the  $E^2$  term had little impact on our results  
476 (**Supplementary Table 15**), suggesting that nonlinear effects do not greatly impact our findings.  
477 Eighth, we have analyzed British-ancestry samples from the UK Biobank, but an important  
478 future direction is to extend our analyses to cohorts of diverse genetic ancestry<sup>52,53</sup>, which may  
479 differ in their distributions of E variables, tagging of causal E variables by measured E variables,  
480 and/or causal GxE effects (analogous to differences in main G effects<sup>45,54</sup>). Eighth, we do not  
481 analyze GxAge interaction (and we note the limited age variation in UK Biobank samples; age =  
482  $55 \pm 8$  years), but we highlight GxAge interaction and longitudinal data as important directions  
483 for future research<sup>51,55,56</sup>. Despite these limitations, our work quantifies and distinguishes three  
484 different types of GxE interaction across a broad set of traits and E variables.

485

#### 486 **Code Availability**

487

488 Cross trait LDSC: <https://github.com/bulik/ldsc>

489 BOLT-LMM: <https://alkesgroup.broadinstitute.org/BOLT-LMM/downloads/>

490 PRSxE regression: Will be added upon publication.

491 Code to reproduce analysis: Will be added upon publication.

492

#### 493 **Data Availability**

494

495 We will make the results of the three statistical approaches we use here publicly available upon  
496 publication.

497

#### 498 **Acknowledgements**

499

500 We are grateful to Martin Zhang, Ben Strober, Xilin Jiang, and Jordan Rossen for helpful  
501 discussions and Sriram Sankararaman and Ali Pazokitoroudi for comments on an earlier version  
502 of this manuscript. This research was conducted using the UK Biobank resource under  
503 application no. 16549 and funded by National Institutes of Health (NIH) grants R01 MH101244,  
504 R37 MH107649 and R01 HG006399. The funders had no role in study design, data collection  
505 and analysis, decision to publish or preparation of the manuscript.

506

## 507 **Methods**

508

### 509 *Data sources and preprocessing*

510

511 We used data from the UK Biobank in all our analyses. For polygenic score-based analyses that  
512 required a training and testing dataset, we used a set of 337K unrelated white British individuals  
513 for training<sup>27</sup>. For testing, we used a set of 49K European individuals who are unrelated to each  
514 other and to the training cohort<sup>27</sup>. Note that while “testing” typically refers to a setting where the  
515 ultimate goal is to assess PRS accuracy, here we use it to refer to the set of samples we in which  
516 we run a regression of phenotype on PRSxE and covariates. We used polygenic scores generated  
517 by ref.<sup>27</sup>. We used the linear scoring function in Plink v1.9<sup>57</sup> to compute polygenic scores in the  
518 set of 49K test individuals.

519

### 520 *Choice of traits and environmental variables*

521

522 We chose a set of 33 traits with SNP heritability Z scores > 6 and squared genetic correlation less  
523 than 0.5 (**Supplementary Table 3, Supplementary Table 4**). We chose a set of 10 E variables,  
524 including 5 previously analyzed E variables from ref.<sup>14</sup> and 5 additional E variables (Air  
525 pollution, time spent napping, sleeplessness, Diet, wheat consumption) (**Supplementary Figure**  
526 **5**).

527

528 To compute the Diet variable, we performed PCA on a covariance matrix consisting of several  
529 diet variables: cooked vegetable intake, salad intake, fresh fruit intake, processed meat intake,  
530 poultry intake, beef intake, pork intake, coffee intake (**Supplementary Figure 7**). We used the  
531 function `prcomp` in R and extracted the first PC.

532

### 533 *Genetic correlation approach to detecting GxE*

534

535 We performed GWAS using BOLT-LMM<sup>26</sup> within bins of E variables. Then, we used bivariate  
536 LD Score regression<sup>36</sup> to estimate the genetic correlation between the top and bottom quintiles of  
537 E variables; for binary E variables, we estimated the genetic correlation between individuals in  
538 each E bin. We used imputed SNPs with MAF > 0.01% and used the `--no-intercept` option to  
539 increase our power. Computed a Z score testing against the null hypothesis that the genetic  
540 correlation is 1 as:

541

$$Z = \frac{1 - \hat{r}_g}{\widehat{se}}$$

542

### 543 *PRSxE regression approach to detecting GxE*

544  
545  
546

Our PRSxE regression takes the following form:

$$Y = PRS + E + PRS * E + C\#$$

547  
548  
549  
550  
551  
552  
553  
554  
555

where Y is the trait value, PRS is the polygenic score for the trait (see *Data sources and preprocessing*), E is the environment variable, and C is a set of covariates. For all analyses, we correct for the following covariates: age, sex, 10 genetic PCs computed in the held-out set, the squared E variable:  $E^2$ , age\*sex, E\*age, E\*sex. We carried out this regression using the Python package statsmodels v0.14. We also compute a ‘base’ model, which is the same regression without the PRSxE term. We use the p-value associated with the PRSxE term in the interaction model to assess significance.

556  
557  
558

To test whether our results were driven by heteroskedasticity, we performed the same analysis using robust standard errors as implemented in statsmodels using the ‘H1’ covariance matrix (**Supplementary Table 12**).

559  
560  
561  
562

We note the PRSxE regression test is not expected to produce a significant finding if the environmental variance changes as a function of E but the genetic variance does not change as a function of E, because the PRS does not measure changes in environmental variance.

563  
564

*SNP-heritability by E approach to detecting GxE*

565  
566  
567  
568

We used BOLT-REML<sup>33</sup> v2.3.6 to compute heritability in bins of E variables. To test for a significant difference in heritability between two bins, we computed a Z score as:

$$Z = \frac{h_1^2 - h_2^2}{\sqrt{\sigma_1^2 + \sigma_2^2}}$$

569

where 1 and 2 index the E bins.

570

571

*False Discovery Rate (FDR) control*

572

573

574

575

576

577

578

579

580

581

582

583

584

585

586

We chose a 5% FDR control separately for each statistical approach (Genetic correlation, PRSxE regression, and SNP-heritability by E) using the qvalue R package<sup>58</sup>. We ensured our one-sided test against a null genetic correlation of 1 did not produce a skewed P-value distribution, which could indicate improper choice of a one-sided test. We chose to control the FDR separately for GxE and GxSex analyses because we expected the proportional of truly null tests to be different between GxE and GxSex. In particular, we expected to find more truly positive GxSex tests given previous studies<sup>22,24</sup>. Consistent with this, we found the qvalue procedure for estimating the proportion of truly null hypotheses failed in the GxSex analyses and we had to set the proportion of true null tests ( $\pi_0$ ) to 1, which is equivalent to the Benjamini-Hochberg procedure<sup>59</sup>. Story and Tibshirani<sup>60</sup> argue this is much more conservative than the qvalue procedure. Our choice to control each E variable together is conservative, but accounts for non-zero correlations between E variables.

*Classification of trait-E pairs into Scenarios*

587  
588 We combined the results of the three statistical approaches to classify trait-E pairs into 3 distinct  
589 scenarios. We classified trait-E pairs into Scenario 1 if the Genetic correlation was significantly  
590 less than 1. We classified trait-E pairs into Scenario 2 if the SNP-heritability by E and PRSxE  
591 regression approaches were significant. We classified trait-E pairs into Scenario 3 if the PRSxE  
592 regression approach was significant but the SNP-heritability by E approach was not significant.  
593 It is possible that the SNP-heritability by E approach is significant but the PRSxE regression  
594 approach is not significant, which should not be viewed as an instance of GxE because the SNP-  
595 heritability difference may be driven by changes to the environmental variance rather than the  
596 genetic variance. In addition, it is possible for trait-E pairs to be classified into both Scenario 1  
597 and Scenario 2, or both Scenario 1 and Scenario 3, but not both Scenario 2 and Scenario 3  
598 because significance or non-significance of the SNP-heritability by E approach are mutually  
599 exclusive.

600

### 601 *Scalability of statistical approaches*

602

603 We consider the scalability of the three statistical approaches we use here. First, there is the  
604 computational cost of producing the input to our statistical approaches. For the genetic  
605 correlation test, this consists of running GWAS in bins of E variables. There are many scalable  
606 approaches for this, including BOLT-LMM<sup>26</sup>, regenie<sup>61</sup>, and fastGWA<sup>62</sup>. For PRSxE regression,  
607 this consists of computing PRS weights. There are many scalable approaches for this including  
608 BOLT-LMM<sup>26</sup>, PRScs<sup>63</sup>, SBayesR<sup>64</sup>, and LDpred2<sup>65</sup>. SNP-heritability by E does not require  
609 generating additional input. In these analyses, we use BOLT-LMM for GWAS, which has a  
610 runtime that scales with  $O(MN)$ , where  $M$  is the number of SNPs and  $N$  is the sample size of  
611 individuals. For PRSxE regression we use weights computed by Weissbrod et al 2022<sup>27</sup>, who did  
612 not publish an analysis of runtime. Second, there is the computational cost of the statistical  
613 approaches themselves. For genetic correlation, we use cross-trait LDSC<sup>25</sup>, which runs in  
614 seconds ( $< 30$ s for the SNP sets that we analyze here). For PRSxE regression, we use a multiple  
615 regression, which also runs in seconds ( $< 30$ s for the sample size that we analyze here). For SNP-  
616 heritability by E, we use BOLT-REML<sup>33</sup>, which has a runtime that scales with  $O(MN)$ .

617

### 618 *Simulations*

619

620 To test the power of each approach, we simulated 1,000 replicates of each scenario. In all cases,  
621 we simulated two E bins and varied the parameters according to the respective generative  
622 models. For each replicate, we simulated  $M=10,000$  causal SNPs with effect sizes drawn from a  
623 specified distribution. We generated unlinked genotypes with binomial sampling from an allele  
624 frequency of 0.5.

625

626 We simulated causal effect sizes for each scenario as follows:

627

628 Scenario 1

$$\begin{bmatrix} \beta_1 \\ \beta_2 \end{bmatrix} \sim N \left( \begin{bmatrix} 0 \\ 0 \end{bmatrix}, \begin{bmatrix} \sigma_g^2/M & \gamma/M \\ \gamma/M & \sigma_g^2/M \end{bmatrix} \right)$$

629

630 We simulated  $\sigma_g^2 = 0.25$  and varied  $\gamma$  to produce genetic correlations  
 631  $r_g \in \{1, 0.99, 0.98, 0.97, 0.96, 0.95, 0.94\}$ .

632  
 633 Scenario 2

$$\begin{bmatrix} \beta_1 \\ \beta_2 \end{bmatrix} \sim N \left( \begin{bmatrix} 0 \\ 0 \end{bmatrix}, \begin{bmatrix} \sigma_{g,1}^2/M & \sigma_{g1}\sigma_{g2}/M \\ \sigma_{g1}\sigma_{g2}/M & \sigma_{g,2}^2/M \end{bmatrix} \right)$$

634  
 635  
 636 We simulated  $\sigma_{g1}^2=0.25$  and set  $\sigma_{g2}^2$  to produce a difference in heritability:  
 637  $\{0, 0.01, 0.02, 0.03, 0.04, 0.05\}$ . Our choice of covariance ensures the genetic correlation is one.

638  
 639 Scenario 3  
 640

$$\begin{bmatrix} \beta_1 \\ \beta_2 \end{bmatrix} \sim N \left( \begin{bmatrix} 0 \\ 0 \end{bmatrix}, \begin{bmatrix} \sigma_g^2/M & \sigma_g^2/M \\ \sigma_g^2/M & \sigma_g^2/M \end{bmatrix} \right)$$

641  
 642 We set  $\sigma_g^2 = 0.25$ . To simulate proportional amplification, we multiplied the phenotypes for  
 643 individuals in environment 2 by a constant:  $\{1.0, 1.025, 1.05, 1.075, 1.1\}$ .

644  
 645 Using the simulated causal effect sizes, we simulated GWAS effect size estimates as:

$$\widehat{\beta}_1 \sim N\left(\beta_1, \frac{(1-h_1^2)/M}{N}\right)$$

$$\widehat{\beta}_2 \sim N\left(\beta_2, \frac{(1-h_2^2)/M}{N}\right)$$

646  
 647  
 648 where 1 and 2 index the environments and  $N$  denotes GWAS sample size. We estimate  $h_g^2$  from  
 649 the simulated causal effect sizes by first computing the  $\chi^2$  statistic ( $\chi^2 := N * \widehat{\beta}^2$ ), then  
 650 computing  $h_g^2 = \frac{M}{N} E[\chi^2 - 1]$ , where  $E$  denotes the mean computed over the independent  
 651 SNPs<sup>25</sup>.

652  
 653 We compute the genetic correlation as:

$$r_g = \frac{\widehat{\beta}_1^T \widehat{\beta}_2}{\sqrt{\widehat{h}_{g,1}^2 * \widehat{h}_{g,2}^2}}$$

654  
 655 where  $T$  denotes the transpose. We compute standard errors for the estimates using a jackknife  
 656 over SNPs, where we leave out one SNP at a time because they are independent.

657  
 658 To simulate PRSxE, we first simulated causal effect sizes for 10,000 independent SNPs. Then,  
 659 we compute PRS weights analytically as:

$$\beta_{PRS} = \left( \frac{h_g^2}{h_g^2 + \frac{M}{N}} \right) \widehat{\beta}.$$

661  
662 This simple shrinkage estimator can be interpreted as the posterior mean causal effect size under  
663 a normal prior (in the special case of no LD), and is similar to the posterior mean causal effect  
664 size under a point-normal prior (in the special case of no LD) when the genetic architecture is  
665 highly polygenic<sup>66</sup>, as simulated here.

666  
667 We estimate  $h_g^2$  without knowledge of the E bins, mimicking estimation of SNP-heritability  
668 across the 337K individuals; we estimate  $h_g^2$  as the sum of squared standardized effect sizes  
669 (averaged across E bins).

670  
671 We also evaluated the performance of GxEMM in detecting GxE in Scenarios 1, 2, and 3. We  
672 followed the simulation framework in the original publication and simulated 1,000 causal SNPs  
673 and 10,000 individuals. We simulated a binary E variable and drew SNP effects according to  
674 each Scenario. We performed two tests within the GxEMM framework: 1) IID versus Hom,  
675 which tests for polygenic GxE under homoscedasticity, and 2) Free versus Hom, which test for  
676 polygenic GxE allowing for heteroskedasticity. We performed a Wald test as implemented in  
677 GxEMM and compared the point estimates of heritability in the free model to the simulated  
678 heritability in each of the environments. We performed 100 simulation replicates.

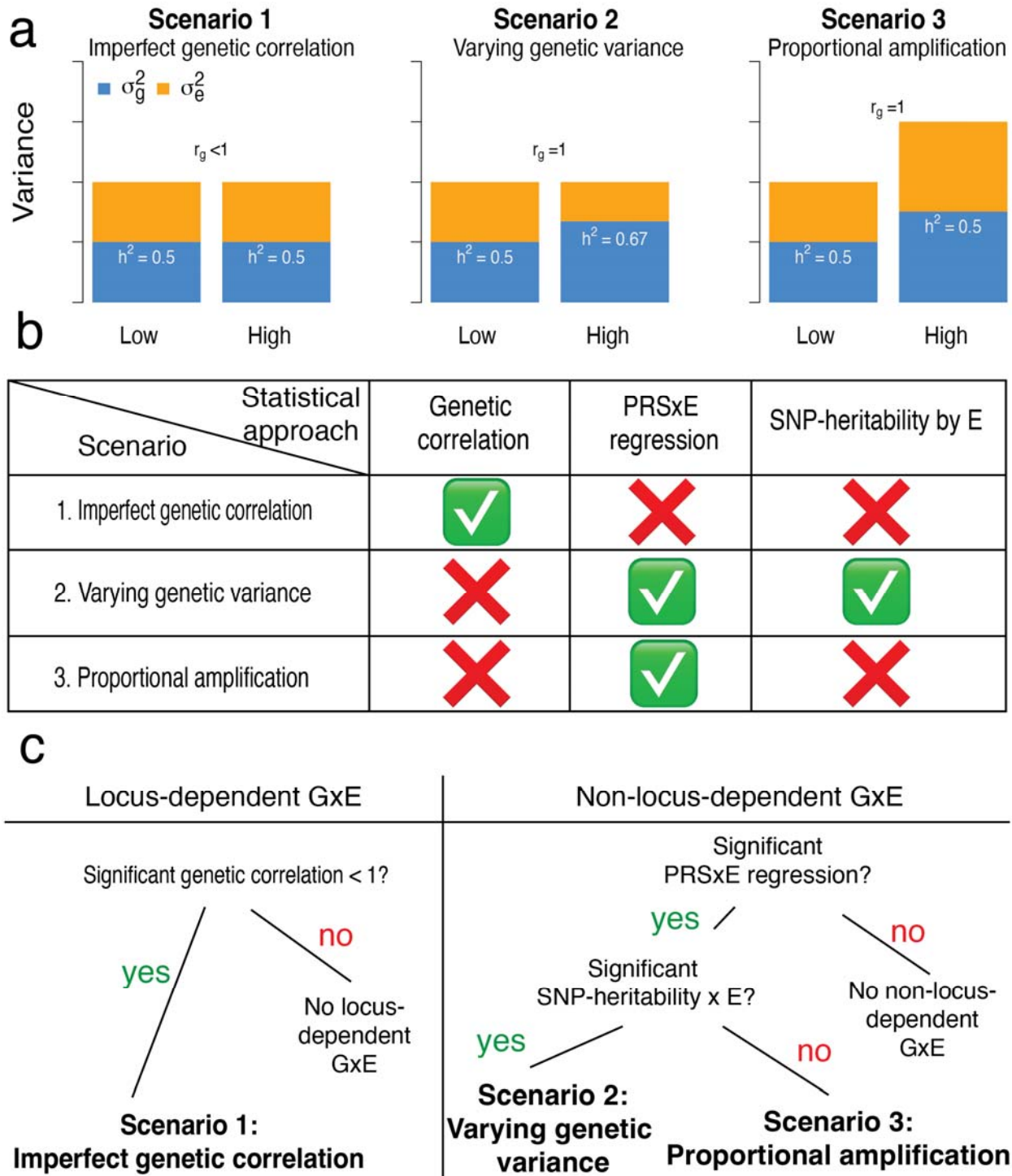
679  
680 To compare GxEMM with our tests, we simulated data under the same framework with matched  
681 sample sizes. Specifically, for genetic correlation and SNP-heritability x E, we simulated 5,000  
682 individual per E bin (total N=10,000). For PRSxE, we used a training set sample size of 337K,  
683 which matches the real data, and a held out set of N=10,000.

684  
685 *Estimation of trait variance explained*

686  
687 For trait-E pairs in Scenario 1, we compute the trait variance explained by GxE as  $(1 - r_g)/2$  for  
688 binary E variables (where  $r_g$  is the genetic correlation between the two E bins) (**Supplementary**  
689 **Note**) and  $\frac{1-r_g}{10}$  for continuous E variables (where  $r_g$  is the genetic correlation between the top  
690 and bottom quintiles of E values). To obtain the transformation for continuous E variables, we  
691 used our simulations (see above) to examine the relationship between estimated genetic  
692 correlation and the variance explained by GxE. We found when we binned the E variable into 5  
693 bins and computed the genetic correlation between the top and bottom bins, the transformation  
694  $\frac{1-r_g}{10}$  produced accurate estimates of the variance explained by GxE. For trait-E pairs in Scenarios  
695 2 or 3, we divide the variance explained by the PRSxE regression term by the variance explained  
696 by the PRS and multiply by the SNP-heritability. We verified these scaling procedures produce  
697 accurate estimates of the excess variance explained by GxE in simulations (**Supplementary**  
698 **Figure S4**). For Scenario 1, we simulated a continuous E variable with mean 0 and variance 1  
699 for 337K individuals. We simulated main genetic effects drawn from a normal distribution with  
700 mean 0 and variance 0.25 and environment interaction effects from a normal distribution with  
701 mean 0 and variance across a range of parameters (1e-1 to 1e-5) for 5,000 SNPs. We binned  
702 individuals into 5 bins and ran a GWAS in the top and bottom bins and compute the genetic  
703 correlation between the bins. Then, we scaled the estimates according to the formula above  
704 (**Supplementary Figure S4a**). For Scenarios 2 and 3, we simulated 1,000 causal SNPs from a  
705 normal distribution with mean 0 and variance 0.25. We simulated a continuous E variable with

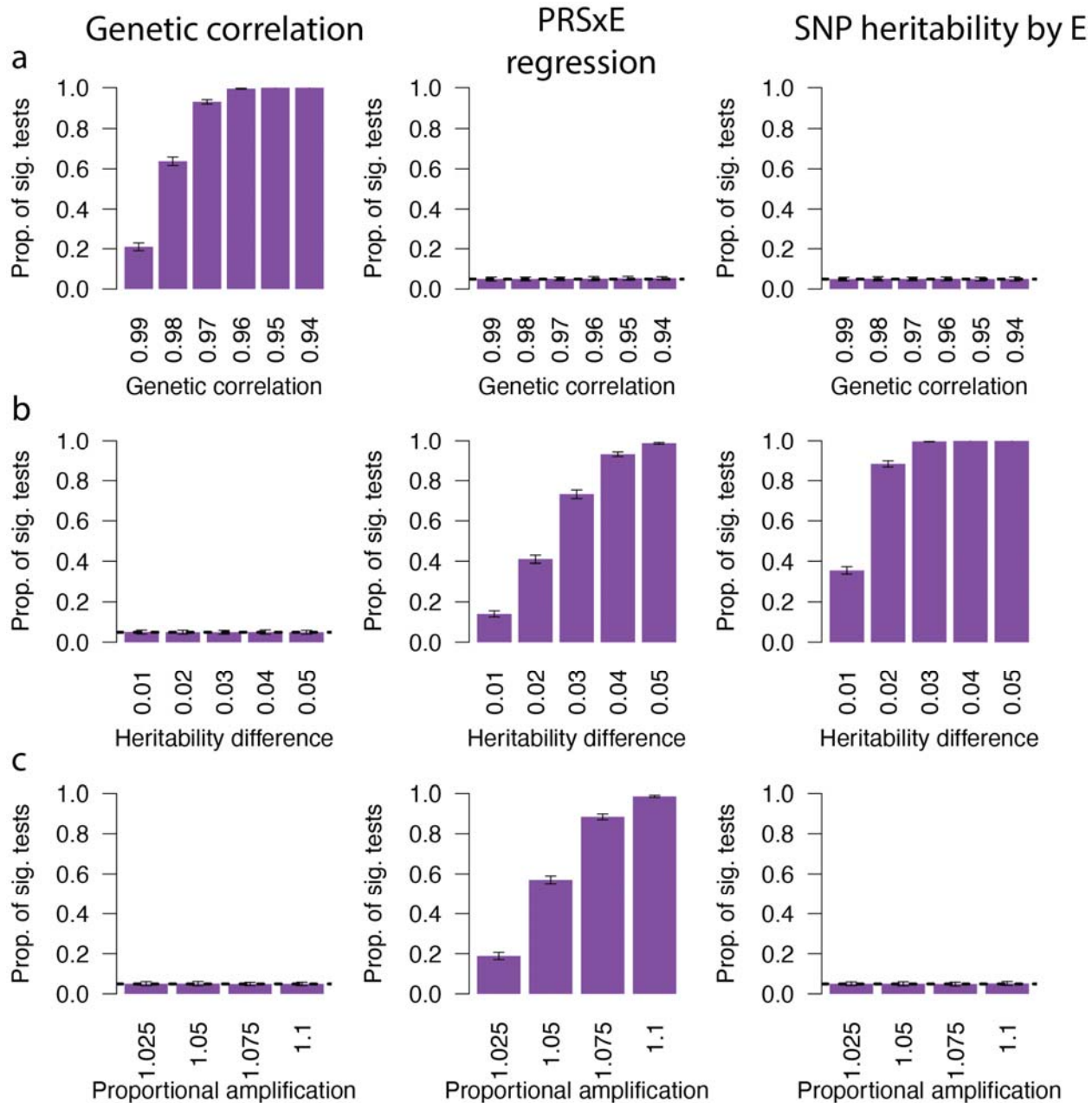


706 mean 0 and variance 1 for 49K individuals. We set the amplification parameter to 0.1 and  
707 generated phenotypes according to Eq. 1 (*Overview of methods*). We performed GWAS and  
708 estimated PRS weights as in the *Simulations* section. Then, we ran the PRSxE test and computed  
709 the variance explained. We then compared this to the true variance explained (**Supplementary**  
710 **Figure S4b, S4c**). This scaling assumes that PRSxE effects linearly extrapolate to GxE effects.  
711 We do not use the estimates of differences in SNP-heritability by E to estimate the variance  
712 explained by GxE. When reporting average variance explained per trait, we computed the  $R^2$  for  
713 each trait using a model including all marginally significant (FDR < 5%) interaction terms for  
714 that trait (**Supplementary Table 14**).

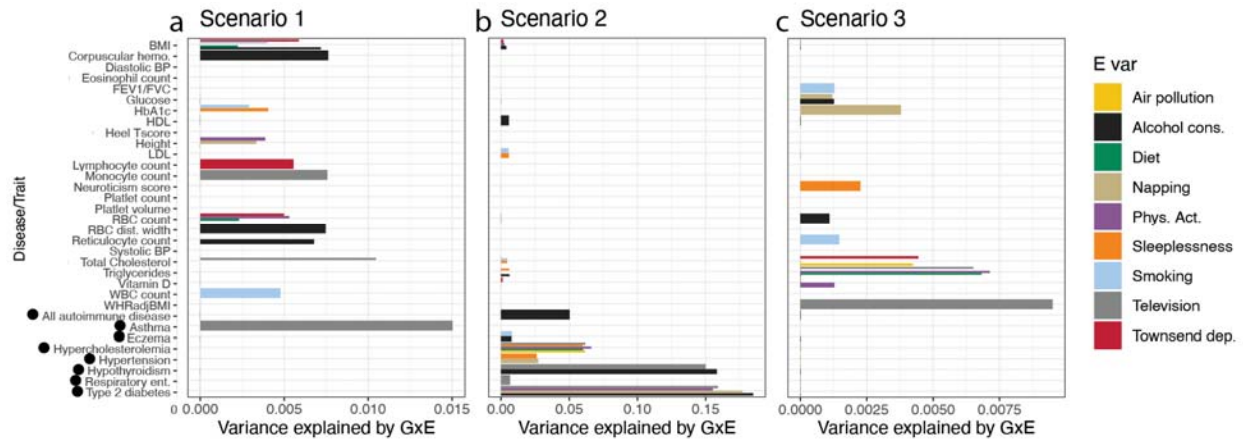


715  
716  
717  
718  
719

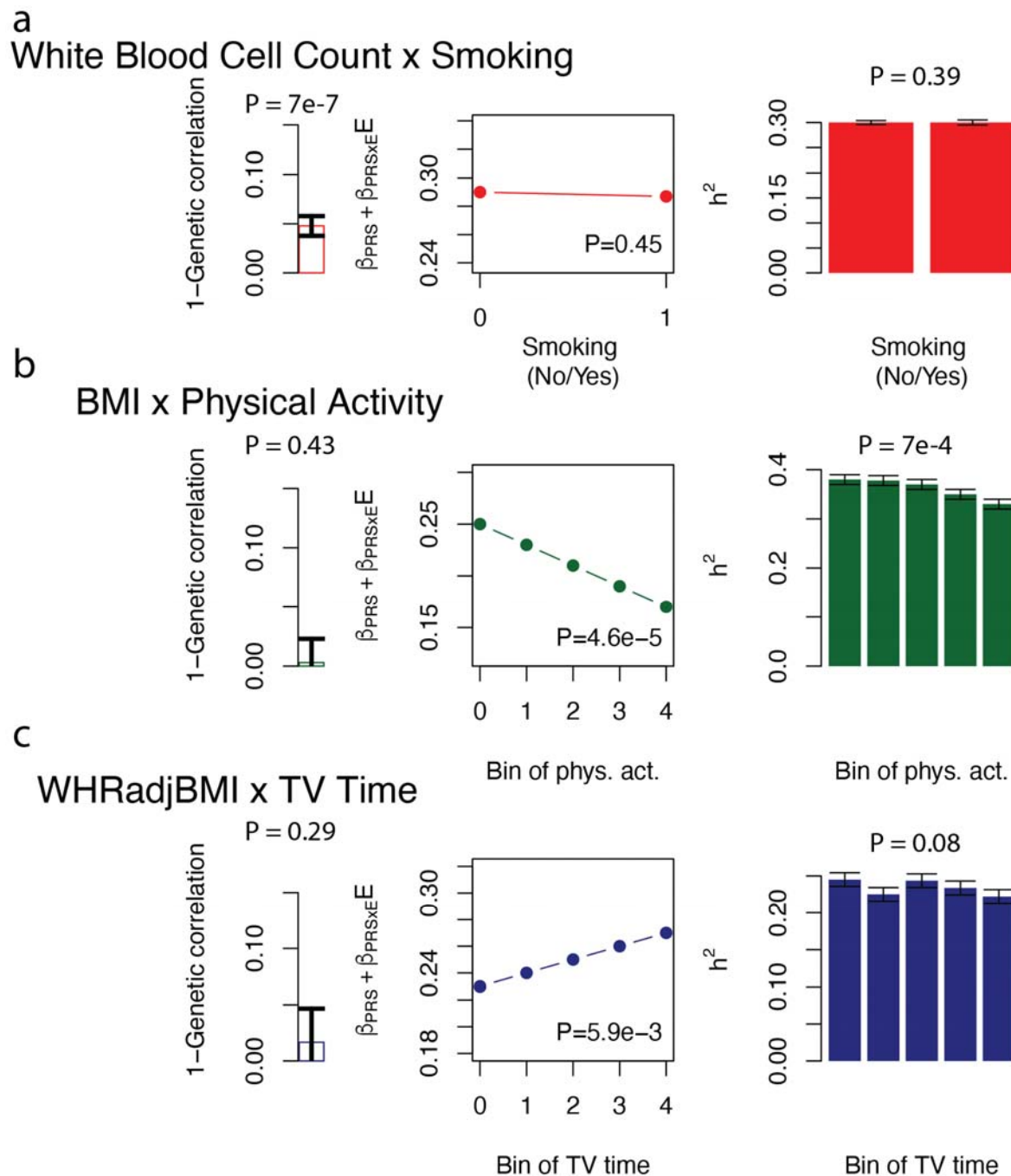
**Figure 1. Overview of 3 GxE Scenarios and statistical approaches to detect and distinguish between them.** (a) Relative values of genetic (blue) and environmental (orange) variance in each Scenario. (b) Statistical approaches to detect and distinguish between each Scenario. (c) Flow chart for classifying results into Scenarios.



720  
 721 **Figure 2. Detecting and distinguishing between 3 Scenarios of GxE interaction in**  
 722 **simulations.** Rows denote 3 Scenarios (1-3), and columns denote 3 statistical approaches. (a)  
 723 Proportion of significant tests for Scenario 1 (Imperfect genetic correlation) across 3 statistical  
 724 approaches. (b) Proportion of significant tests for Scenario 2 (varying genetic variance) across 3  
 725 statistical approaches. (c) Proportion of significant tests for Scenario 3 (proportional  
 726 amplification) across 3 statistical approaches. Error bars denote standard deviations across 100  
 727 simulation replicates. Numerical results are reported in **Supplementary Table 1**.  
 728

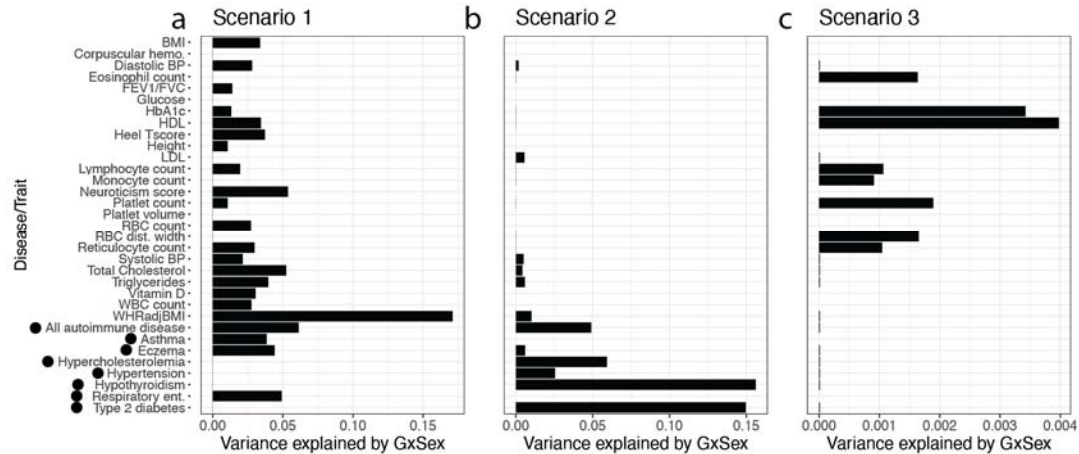


729  
 730 **Figure 3. Detecting, quantifying, and distinguishing between 3 Scenarios of GxE**  
 731 **interaction across 33 traits and 10 E variables.** Traits are listed on the y-axis and estimates of  
 732 excess variance explained by GxE are reported on the x-axis. Only significant results are  
 733 reported (FDR < 5% across traits and E variables, computed separately for each Scenario). For  
 734 traits with multiple significant E variables in a given Scenario, results for each significant E  
 735 variable are reported separately using bars with smaller thickness. Disease traits are denoted with  
 736 black dots. (a) Results for trait-E pairs in Scenario 1: Imperfect genetic correlation. (b) Results  
 737 for trait-E pairs in Scenario 2: Varying genetic variance; we note that BMI has significant GxE  
 738 for Townsend deprivation (red), physical activity (purple), and alcohol consumption (black). (c)  
 739 Results for trait-E pairs in Scenario 3: Proportional amplification. Numerical results are reported  
 740 in **Supplementary Table S5**.



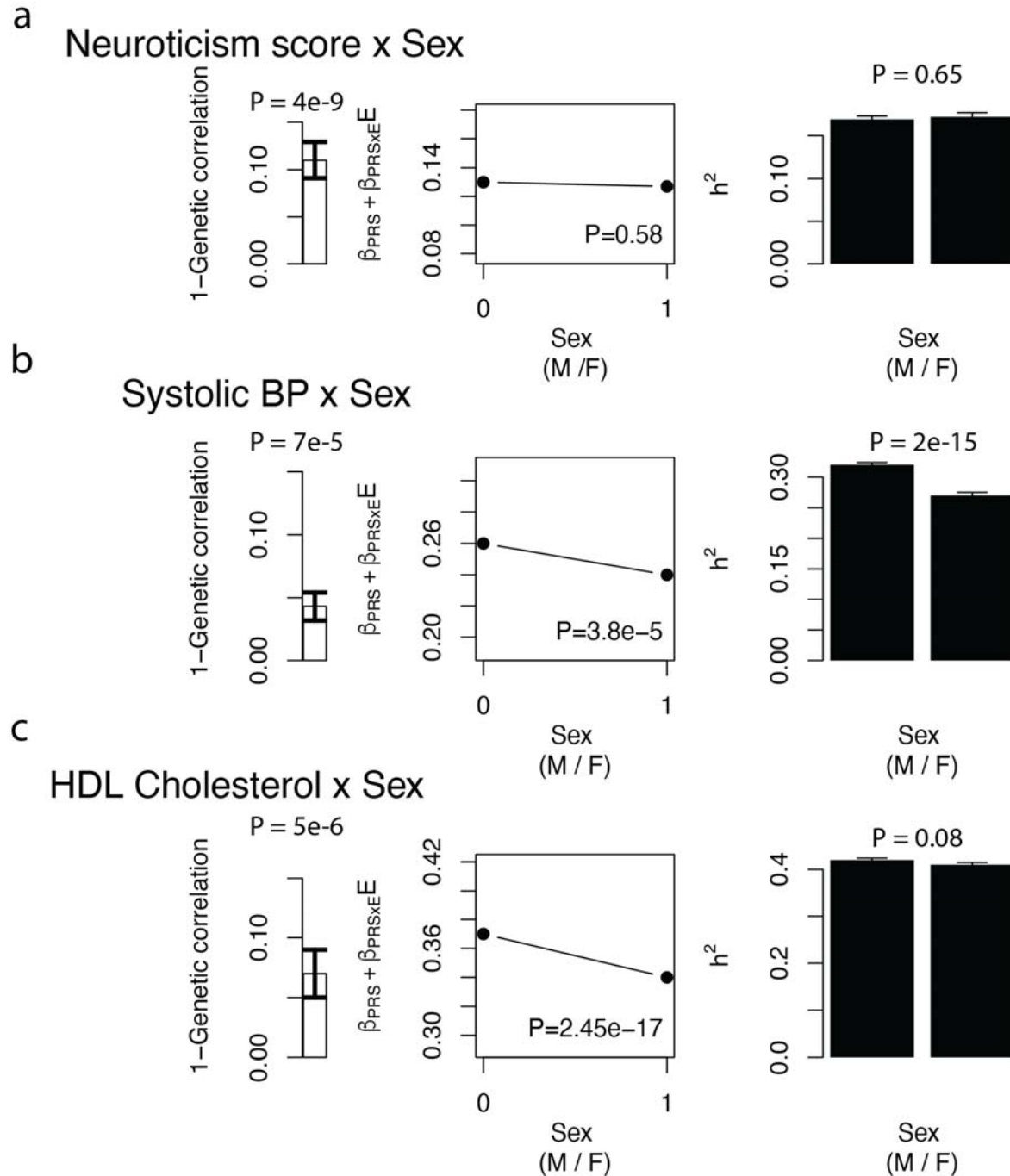
741  
742 **Figure 4. Examples of 3 Scenarios of GxE interaction.** (a) White blood cell count x smoking  
743 status is consistent with Scenario 1: Imperfect genetic correlation. (b) BMI x physical activity is  
744 consistent with Scenario 2: Varying genetic variance. (c) Waist-to-hip ratio adjusted for BMI x  
745 Time spent watching TV is consistent with Scenario 3: Proportional amplification. Numerical  
746 results are reported in **Supplementary Table S8**.

747  
748  
749



750  
751  
752  
753  
754  
755  
756  
757  
758  
759

**Figure 5. Detecting, quantifying, and distinguishing between 3 Scenarios of GxSex interaction across 33 traits.** Traits are listed on the y-axis and estimates of excess variance explained by GxSex are reported on the x-axis. Only significant results are reported (FDR < 5% across traits, computed separately for each Scenario). Disease traits are denoted with black dots. (a) Results for traits in Scenario 1: Imperfect genetic correlation. (b) Results for traits in Scenario 2: Varying genetic variance. (c) Results for traits in Scenario 3: Proportional amplification. Numerical results are reported in **Supplementary Table S9**.



760  
 761 **Figure 6. Examples of 3 Scenarios of GxSex interaction.** (a) Neuroticism score x Sex is  
 762 consistent with Scenario 1: Imperfect genetic correlation. (b) Systolic blood pressure x Sex is  
 763 consistent with Scenario 1 and Scenario 2. (c) HDL Cholesterol x Sex is consistent with Scenario  
 764 1 and Scenario 3. Numerical results are reported in **Supplementary Table S11**.  
 765

766 **References**

- 767 1. Hunter, D. J. Gene–environment interactions in human diseases. *Nat. Rev. Genet.* **6**, 287–298  
768 (2005).
- 769 2. Thomas, D. Gene-Environment-Wide Association Studies: Emerging Approaches. *Nat. Rev.*  
770 *Genet.* **11**, 259–272 (2010).
- 771 3. Franks, P. W. & McCarthy, M. I. Exposing the exposures responsible for type 2 diabetes and  
772 obesity. *Science* **354**, 69–73 (2016).
- 773 4. Li, J., Li, X., Zhang, S. & Snyder, M. Gene-Environment Interaction in the Era of Precision  
774 Medicine. *Cell* **177**, 38–44 (2019).
- 775 5. Hu, Z. *et al.* A genome-wide association study identifies two new lung cancer susceptibility  
776 loci at 13q12.12 and 22q12.2 in Han Chinese. *Nat. Genet.* **43**, 792–796 (2011).
- 777 6. Wu, C. *et al.* Genome-wide association analyses of esophageal squamous cell carcinoma in  
778 Chinese identify multiple susceptibility loci and gene-environment interactions. *Nat. Genet.*  
779 **44**, 1090–1097 (2012).
- 780 7. Young, A. I., Wauthier, F. & Donnelly, P. Multiple novel gene-by-environment interactions  
781 modify the effect of FTO variants on body mass index. *Nat. Commun.* **7**, 12724 (2016).
- 782 8. Yang, J. *et al.* FTO genotype is associated with phenotypic variability of body mass index.  
783 *Nature* **490**, 267–272 (2012).
- 784 9. Shungin, D. *et al.* Ranking and characterization of established BMI and lipid associated loci as  
785 candidates for gene-environment interactions. *PLOS Genet.* **13**, e1006812 (2017).
- 786 10. Young, A. I., Wauthier, F. L. & Donnelly, P. Identifying loci affecting trait variability  
787 and detecting interactions in genome-wide association studies. *Nat. Genet.* **50**, 1608–1614  
788 (2018).



- 789 11. Wang, H. *et al.* Genotype-by-environment interactions inferred from genetic effects on  
790 phenotypic variability in the UK Biobank. *Sci. Adv.* **5**, eaaw3538 (2019).
- 791 12. Westerman, K. E. *et al.* Variance-quantitative trait loci enable systematic discovery of  
792 gene-environment interactions for cardiometabolic serum biomarkers. *Nat. Commun.* **13**, 3993  
793 (2022).
- 794 13. Yang, J., Lee, S. H., Goddard, M. E. & Visscher, P. M. GCTA: a tool for genome-wide  
795 complex trait analysis. *Am. J. Hum. Genet.* **88**, 76–82 (2011).
- 796 14. Robinson, M. R. *et al.* Genotype–covariate interaction effects and the heritability of adult  
797 body mass index. *Nat. Genet.* **49**, 1174–1181 (2017).
- 798 15. Moore, R. *et al.* A linear mixed-model approach to study multivariate gene–environment  
799 interactions. *Nat. Genet.* **51**, 180–186 (2019).
- 800 16. Dahl, A. *et al.* A Robust Method Uncovers Significant Context-Specific Heritability in  
801 Diverse Complex Traits. *Am. J. Hum. Genet.* **106**, 71–91 (2020).
- 802 17. Kerin, M. & Marchini, J. Inferring Gene-by-Environment Interactions with a Bayesian  
803 Whole-Genome Regression Model. *Am. J. Hum. Genet.* **107**, 698–713 (2020).
- 804 18. Di Scipio, M. *et al.* A versatile, fast and unbiased method for estimation of gene-by-  
805 environment interaction effects on biobank-scale datasets. *Nat. Commun.* **14**, 5196 (2023).
- 806 19. Traglia, M. *et al.* Genetic Mechanisms Leading to Sex Differences Across Common  
807 Diseases and Anthropometric Traits. *Genetics* **205**, 979–992 (2017).
- 808 20. Khramtsova, E. A., Davis, L. K. & Stranger, B. E. The role of sex in the genomics  
809 of human complex traits. *Nat. Rev. Genet.* **20**, 173–190 (2019).
- 810 21. Kamitaki, N. *et al.* Complement genes contribute sex-biased vulnerability in diverse  
811 disorders. *Nature* **582**, 577–581 (2020).

- 812 22. Bernabeu, E. *et al.* Sex differences in genetic architecture in the UK Biobank. *Nat. Genet.*  
813 **53**, 1283–1289 (2021).
- 814 23. Khrantsova, E. A. *et al.* Quality control and analytic best practices for testing genetic  
815 models of sex differences in large populations. *Cell* **186**, 2044–2061 (2023).
- 816 24. Zhu, C. *et al.* Amplification is the primary mode of gene-by-sex interaction in complex  
817 human traits. *Cell Genomics* **3**, (2023).
- 818 25. Bulik-Sullivan, B. *et al.* An atlas of genetic correlations across human diseases and traits.  
819 *Nat. Genet.* **47**, 1236–1241 (2015).
- 820 26. Loh, P.-R., Kichaev, G., Gazal, S., Schoech, A. P. & Price, A. L. Mixed-model  
821 association for biobank-scale datasets. *Nat. Genet.* **50**, 906–908 (2018).
- 822 27. Weissbrod, O. *et al.* Leveraging fine-mapping and multipopulation training data to  
823 improve cross-population polygenic risk scores. *Nat. Genet.* **54**, 450–458 (2022).
- 824 28. Rask-Andersen, M., Karlsson, T., Ek, W. E. & Johansson, Å. Gene-environment  
825 interaction study for BMI reveals interactions between genetic factors and physical activity,  
826 alcohol consumption and socioeconomic status. *PLoS Genet.* **13**, e1006977 (2017).
- 827 29. Marderstein, A. R. *et al.* Leveraging phenotypic variability to identify genetic  
828 interactions in human phenotypes. *Am. J. Hum. Genet.* **108**, 49–67 (2021).
- 829 30. Yang, J. *et al.* Common SNPs explain a large proportion of the heritability for human  
830 height. *Nat. Genet.* **42**, 565–569 (2010).
- 831 31. Lee, S. H., Wray, N. R., Goddard, M. E. & Visscher, P. M. Estimating missing  
832 heritability for disease from genome-wide association studies. *Am. J. Hum. Genet.* **88**, 294–  
833 305 (2011).

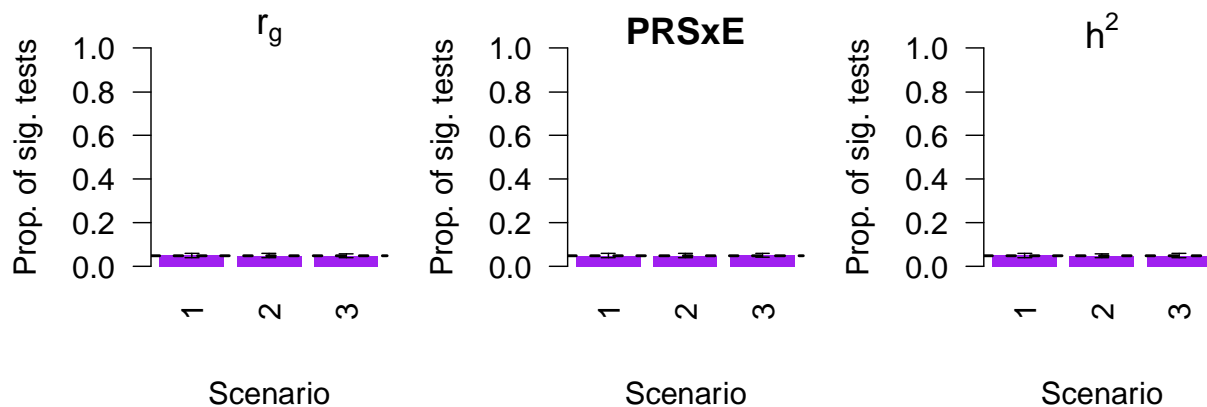
- 834 32. Lee, S. H. *et al.* Estimating the proportion of variation in susceptibility to schizophrenia  
835 captured by common SNPs. *Nat. Genet.* **44**, 247–250 (2012).
- 836 33. Loh, P.-R. *et al.* Contrasting genetic architectures of schizophrenia and other complex  
837 diseases using fast variance-components analysis. *Nat. Genet.* **47**, 1385–1392 (2015).
- 838 34. Pazokitoroudi, A. *et al.* Efficient variance components analysis across millions of  
839 genomes. *Nat. Commun.* **11**, 4020 (2020).
- 840 35. Bycroft, C. *et al.* The UK Biobank resource with deep phenotyping and genomic data.  
841 *Nature* **562**, 203 (2018).
- 842 36. Bulik-Sullivan, B. K. *et al.* LD Score regression distinguishes confounding from  
843 polygenicity in genome-wide association studies. *Nat. Genet.* **47**, 291–295 (2015).
- 844 37. Voorman, A., Lumley, T., McKnight, B. & Rice, K. Behavior of QQ-Plots and Genomic  
845 Control in Studies of Gene-Environment Interaction. *PLOS ONE* **6**, e19416 (2011).
- 846 38. Huber, P. J. The behavior of maximum likelihood estimates under nonstandard  
847 conditions. in *Proceedings of the Fifth Berkeley Symposium on Mathematical Statistics and*  
848 *Probability, Volume 1: Statistics* vol. 5.1 221–234 (University of California Press, 1967).
- 849 39. White, H. A Heteroskedasticity-Consistent Covariance Matrix Estimator and a Direct  
850 Test for Heteroskedasticity. *Econometrica* **48**, 817–838 (1980).
- 851 40. Pedersen, K. M. *et al.* Smoking and Increased White and Red Blood Cells. *Arterioscler.*  
852 *Thromb. Vasc. Biol.* **39**, 965–977 (2019).
- 853 41. Bradbury, K. E., Guo, W., Cairns, B. J., Armstrong, M. E. G. & Key, T. J. Association  
854 between physical activity and body fat percentage, with adjustment for BMI: a large cross-  
855 sectional analysis of UK Biobank. *BMJ Open* **7**, e011843 (2017).

- 856 42. Wendt, F. R. *et al.* Sex-Specific Genetic and Transcriptomic Liability to Neuroticism.  
857 *Biol. Psychiatry* **93**, 243–252 (2023).
- 858 43. Reckelhoff, J. F. Gender Differences in the Regulation of Blood Pressure. *Hypertension*  
859 **37**, 1199–1208 (2001).
- 860 44. Mostafavi, H. *et al.* Variable prediction accuracy of polygenic scores within an ancestry  
861 group. *eLife* **9**, e48376 (2020).
- 862 45. Shi, H. *et al.* Population-specific causal disease effect sizes in functionally important  
863 regions impacted by selection. *Nat. Commun.* **12**, 1098 (2021).
- 864 46. Visscher, P. M., Hill, W. G. & Wray, N. R. Heritability in the genomics era--concepts  
865 and misconceptions. *Nat. Rev. Genet.* **9**, 255–266 (2008).
- 866 47. Polderman, T. J. C. *et al.* Meta-analysis of the heritability of human traits based on fifty  
867 years of twin studies. *Nat. Genet.* **47**, 702–709 (2015).
- 868 48. Zuk, O., Hechter, E., Sunyaev, S. R. & Lander, E. S. The mystery of missing heritability:  
869 Genetic interactions create phantom heritability. *Proc. Natl. Acad. Sci. U. S. A.* **109**, 1193–  
870 1198 (2012).
- 871 49. Cordell, H. J. Detecting gene-gene interactions that underlie human diseases. *Nat. Rev.*  
872 *Genet.* **10**, 392–404 (2009).
- 873 50. Zaitlen, N. *et al.* Informed Conditioning on Clinical Covariates Increases Power in Case-  
874 Control Association Studies. *PLoS Genet.* **8**, e1003032 (2012).
- 875 51. Jiang, X., Holmes, C. & McVean, G. The impact of age on genetic risk for common  
876 diseases. *PLoS Genet.* **17**, e1009723 (2021).
- 877 52. Kanai, M. *et al.* Genetic analysis of quantitative traits in the Japanese population links  
878 cell types to complex human diseases. *Nat. Genet.* **50**, 390–400 (2018).

- 879 53. All of Us Research Program Investigators *et al.* The ‘All of Us’ Research Program. *N.*  
880 *Engl. J. Med.* **381**, 668–676 (2019).
- 881 54. Martin, A. R. *et al.* Clinical use of current polygenic risk scores may exacerbate health  
882 disparities. *Nat. Genet.* **51**, 584 (2019).
- 883 55. Dey, R. *et al.* Efficient and accurate frailty model approach for genome-wide survival  
884 association analysis in large-scale biobanks. *Nat. Commun.* **13**, 5437 (2022).
- 885 56. Pedersen, E. M. *et al.* ADuLT: An efficient and robust time-to-event GWAS. *Nat.*  
886 *Commun.* **14**, 5553 (2023).
- 887 57. Chang, C. C. *et al.* Second-generation PLINK: rising to the challenge of larger and richer  
888 datasets. *GigaScience* **4**, s13742-015-0047–8 (2015).
- 889 58. qvalue: Q-value estimation for false discovery rate control. Storey Lab (2023).
- 890 59. Benjamini, Y. & Hochberg, Y. Controlling the False Discovery Rate: A Practical and  
891 Powerful Approach to Multiple Testing. *J. R. Stat. Soc. Ser. B Methodol.* **57**, 289–300 (1995).
- 892 60. Storey, J. D. & Tibshirani, R. Statistical significance for genomewide studies. *Proc. Natl.*  
893 *Acad. Sci. U. S. A.* **100**, 9440–9445 (2003).
- 894 61. Mbatchou, J. *et al.* Computationally efficient whole-genome regression for quantitative  
895 and binary traits. *Nat. Genet.* **53**, 1097–1103 (2021).
- 896 62. Jiang, L. *et al.* A resource-efficient tool for mixed model association analysis of large-  
897 scale data. *Nat. Genet.* **51**, 1749–1755 (2019).
- 898 63. Ge, T., Chen, C.-Y., Ni, Y., Feng, Y.-C. A. & Smoller, J. W. Polygenic prediction via  
899 Bayesian regression and continuous shrinkage priors. *Nat. Commun.* **10**, 1776 (2019).
- 900 64. Lloyd-Jones, L. R. *et al.* Improved polygenic prediction by Bayesian multiple regression  
901 on summary statistics. *Nat. Commun.* **10**, 5086 (2019).

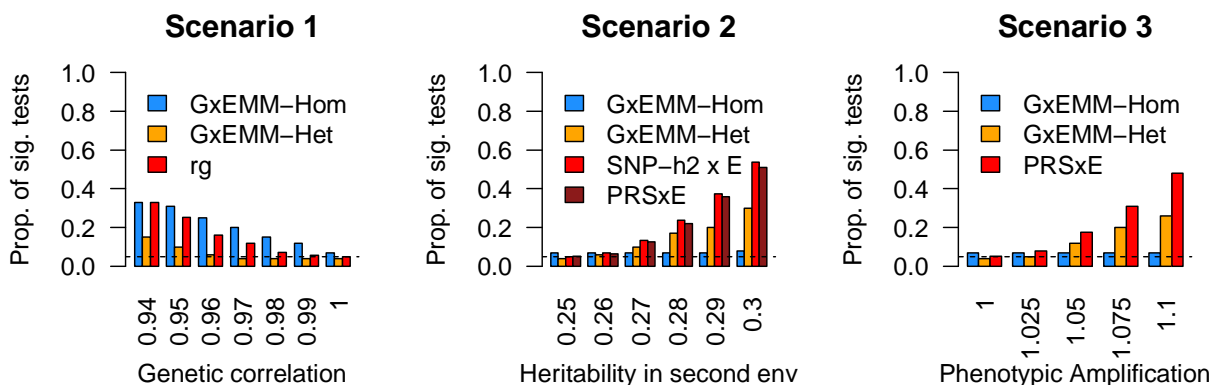
- 902 65. Privé, F., Arbel, J. & Vilhjálmsón, B. J. LDpred2: better, faster, stronger. *Bioinformatics*  
903 **36**, 5424–5431 (2021).
- 904 66. Vilhjálmsón, B. J. *et al.* Modeling Linkage Disequilibrium Increases Accuracy of  
905 Polygenic Risk Scores. *Am. J. Hum. Genet.* **97**, 576–592 (2015).  
906  
907

908  
909 **Supplementary Material**  
910



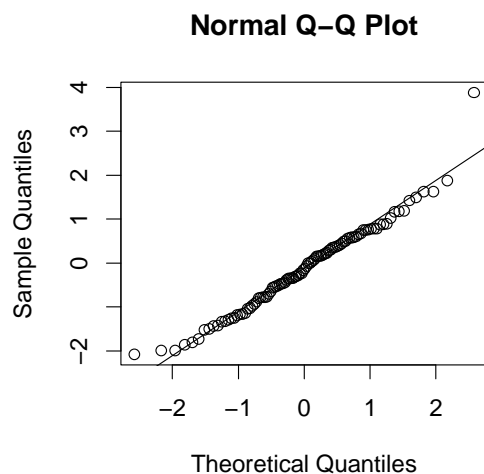
911  
912 **Figure S1 Results of 3 statistical approaches for detecting GxE in null simulations with no**  
913 **GxE.** (a) Proportion of significant tests for genetic correlation across 3 scenarios. (b) Proportion  
914 of significant tests for PRSxE regression across 3 scenarios. (c) Proportion of significant tests for  
915 SNP-heritability by E across 3 scenarios. Error bars denote standard deviations across 100  
916 simulation replicates.

917  
918

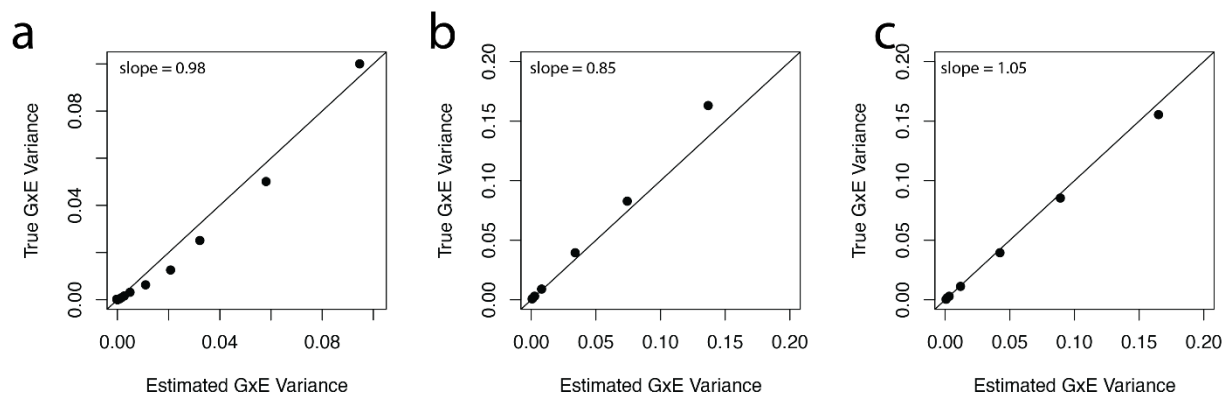


919  
920 **Figure S2 Comparison of three statistical approaches for detecting GxE to ExEMM in**  
921 **simulations.** a) Scenario 1 with varying true genetic correlation across E, b) Scenario 2 with  
922 varying heritability in the second environment, c) Scenario 3 with phenotypic amplification  
923 across E bins.

924

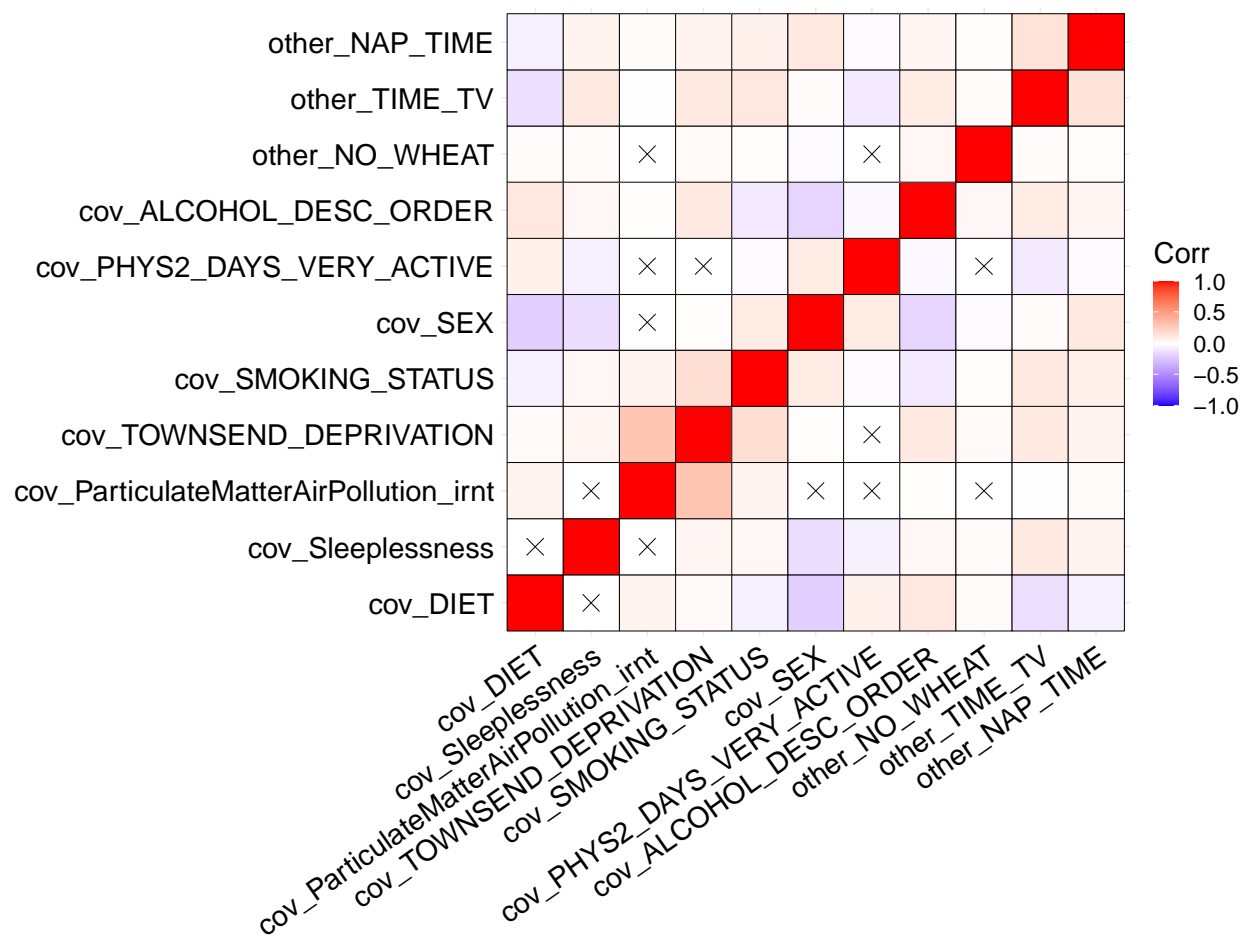


925  
926 **Figure S3 Null simulations of a heritable and genetically correlated E variable.** We  
927 simulated an E variable that is 100% genetically correlated to the phenotype with the same  
928 heritability ( $h^2=25\%$ ). Each point is the result of a PRSxE regression test from a single  
929 simulation (N=100 simulations). We find no inflation of the test statistic under this null model.  
930

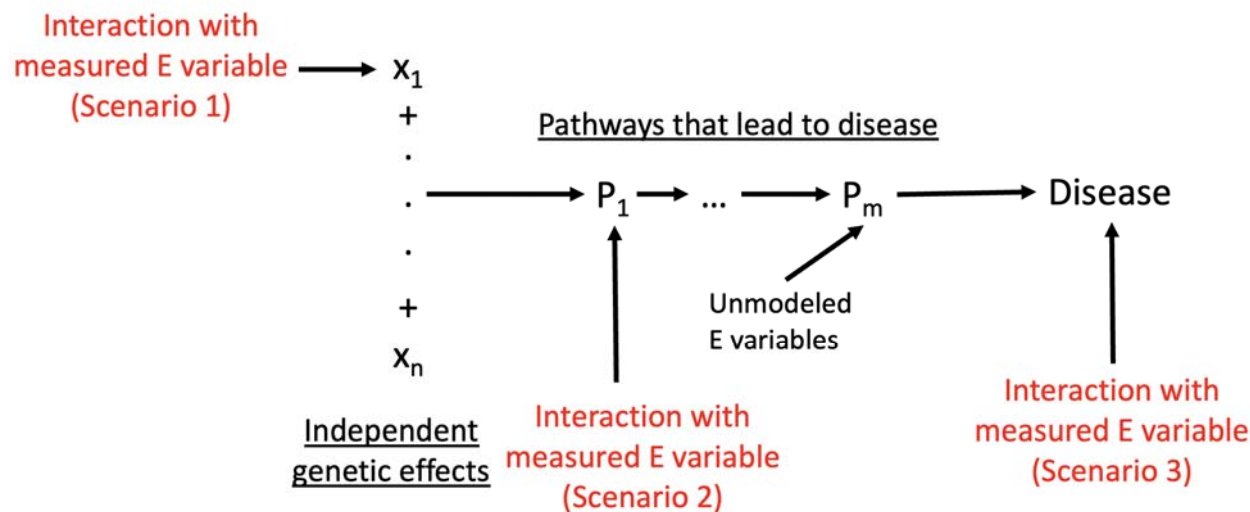


931  
932 **Figure S4 Accuracy of estimates of excess trait variance explained by GxE interaction in**  
933 **simulations.** a) genetic correlation in Scenario 1, b) PRSxE in Scenario 2, and c) PRSxE in  
934 Scenario 3. For all plots, the black line corresponds to the  $y=x$  line and the x and y axes are both  
935 on a log scale.  
936

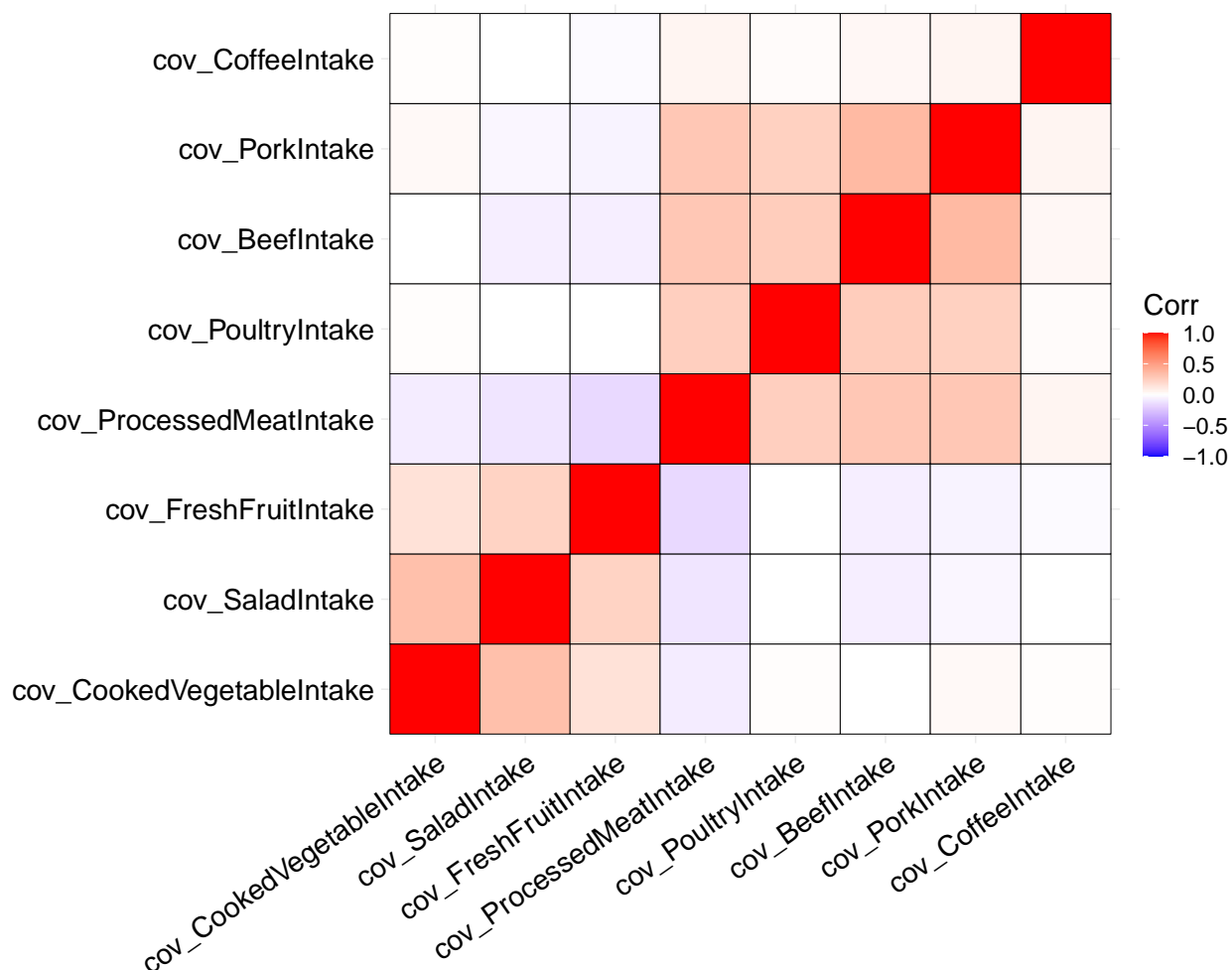




937  
 938 **Figure S5 Phenotypic correlations between E variables.** X denotes non-significant  
 939 comparisons at a p-value threshold of 0.05/11.



940  
 941 **Figure S6 Conceptual model linking three scenarios of GxE.** Scenario 1 can be  
 942 conceptualized as E variables modifying the effects of independent loci. Scenario 2 can be  
 943 conceptualized as modifying pathways which aggregate the genetic effects of many loci,  
 944 resulting in a scaling of genetic effects. Finally, Scenario 3 can be conceptualized as modifying  
 945 the total genetic liability.  
 946



947  
 948 **Figure S7 Phenotypic correlations of diet variables used to construct a composite Diet**  
 949 **variable.** Each cell in the heatmap shows the correlation between the measured diet variable on  
 950 the X axis and the measured diet variable on the Y axis. All correlations are significant at a  
 951 Bonferroni corrected p-value threshold of 0.05.

952  
 953 **Supplementary Table 1 Numerical results of Detecting and distinguishing between 3**  
 954 **Scenarios of GxE interaction in simulations.** For each statistical approach and scenario, we  
 955 report the proportion of significant tests and standard deviation across replicates.

956  
 957 **Supplementary Table 2 Simulations showing bias induced by correlated G and GxE effects.**  
 958 We tested the impact of correlated G and GxE effects on variance component estimates when  
 959 assuming that G and GxE effects are not correlated. We set the true variance of G effects to 0.1  
 960 and the true variance of GxE effects to 0.1. We varied the correlation of the G and GxE effects

961 and simulated values for 100,000 individuals. We estimate the variance explained by G and GxE  
962 using ANOVA in R and report the bias (estimated effect - true effect).

963  
964 **Supplementary Table 3 Description of the 33 UK Biobank traits analyzed.** For each trait we  
965 report a detailed name, the GWAS sample size (including number of cases for binary traits), the  
966 SNP-heritability (liability scale for binary traits), and the PRS accuracy ( $R^2$ ; observed scale for  
967 binary traits).

968  
969 **Supplementary Table 4 SNP-heritability of E variables studied here.** We estimated SNP-  
970 heritability using LDSC. For the composite diet variable, we report the SNP-heritability for each  
971 of the underlying variables that make up the composite diet variable. P-values test against a null  
972 of zero SNP-heritability.

973  
974 **Supplementary Table 5 Numerical results of Detecting, quantifying, and distinguishing**  
975 **between 3 Scenarios of GxE interaction across 33 traits and 10 E variables.** For each trait-E  
976 pair (A, B), we report (C) the excess variance explained by PRSxE and (D) the associated q  
977 value, (E) the difference in heritability between the top and bottom bins of the E variables and  
978 (F) the associated q value, (G) the genetic correlation between the top and bottom bin of the E  
979 variable and (H) the associated q value. We also assign each trait-E pair to the three scenarios (I,  
980 J, K).

981  
982 **Supplementary Table 6 P-values using robust regression in PRSxE regression analysis**  
983 **compared to P-value from the main PRSxE regression analysis.** For each trait-E pair, we  
984 report (A) p-value and (B) effect size for the main PRSxE regression and (C, D) using the Huber-  
985 White variance estimator (robust regression).

986  
987 **Supplementary Table 7 Comparison of disease and quantitative trait variance explained**  
988 **for Scenario 2 GxE.** For 3 matched pairs of disease and quantitative traits, we compared the  
989 variance explained on the observed scale for diseases and quantitative trait scale for quantitative  
990 traits.

991  
992 **Supplementary Table 8 SNP-heritability differences for trait-E pairs with no PRSxE**  
993 **interaction.** For each trait-E pair with a significant difference in SNP-heritability and no  
994 significant PRSxE interaction we report the SNP-heritability difference and q-value at 5% FDR  
995 control.

996  
997 **Supplementary Table 9 Numerical results of Examples of 3 Scenarios of GxE interaction.**  
998 We report detailed results for 3 trait-E pairs reported in Figure 4. For each trait-E pair (A, B), we  
999 report (C) the genetic correlation and (D) p-value, (E) PRSxE regression coefficient and (F) p-  
1000 value, (G, H, I, J, K) SNP-heritability across bins of the E variable with associated standard error  
1001 and (L) the p-value testing for a difference between the top and bottom bins of the E variable.

1002  
1003 **Supplementary Table 10 Numerical results of Detecting, quantifying, and distinguishing**  
1004 **between 3 Scenarios of GxSex interaction across 33 traits.** For each trait (A, B), we report  
1005 (C) the excess variance explained by PRSxSex and (D) the associated q value, (E) the difference  
1006 in heritability between males and females and (F) the associated q value, (G) the genetic

1007 correlation between males and females and (H) the associated q value. We also assign each trait-  
1008 E pair to the three scenarios (I, J, K).

1009  
1010 **Supplementary Table 11 SNP-heritability differences for trait-sex pairs with no PRSxSex**  
1011 **interaction.** For each trait-sex pair with a significant difference in SNP-heritability and no  
1012 significant PRSxSex interaction we report the SNP-heritability difference and q-value at 5%  
1013 FDR control.

1014  
1015 **Supplementary Table 12 Comparison of disease and quantitative trait variance explained**  
1016 **for Scenario 2 GxSex.** For 3 matched pairs of disease and quantitative traits, we compared the  
1017 variance explained on the observed scale for diseases and quantitative trait scale for quantitative  
1018 traits.

1019  
1020 **Supplementary Table 13 Numerical results of Examples of 3 Scenarios of GxSex**  
1021 **interaction.** We report detailed results for 3 trait-sex pairs reported in Figure 4. For each trait (A,  
1022 B), we report (C) the genetic correlation and (D) p-value, (E) PRSxE regression coefficient and  
1023 (F) p-value, (G, H, I, J, K) SNP-heritability across sex with associated standard error and (L) the  
1024 p-value testing for a difference between the top and bottom bins of the E variable.

1025  
1026 **Supplementary Table 14 Average variance explained by binary and quantitative traits.** For  
1027 each scenario, we report the average trait variance explained by binary, quantitative, and all traits  
1028 for both GxE and GxSex interactions.

1029  
1030 **Supplementary Table 15 PRSxE regression results including a non-linear E term.** For each  
1031 trait-E pair, we report (A) P-value and (B) effect size including  $E^2$  as a covariate and (C, D) not  
1032 including  $E^2$  as a covariate.

1033  
1034 **Supplementary Table 16 Trait variance explained by GxE interactions with multiple E**  
1035 **variables.** For traits with multiple marginally significant E variable interactions, we report the  
1036 variance explained by a joint model with all marginally significant E variables.

1037  
1038 **Supplementary Note for “Distinct explanations underlie gene-environment interactions in**  
1039 **the UK Biobank”**